



Biogeochemical response of the Mediterranean Sea to the transient SRES–A2 climate change scenario

Camille Richon^{1,*}, Jean-Claude Dutay¹, Laurent Bopp⁴, Briac Le Vu², James C. Orr¹, Samuel Somot³, and François Dulac¹

¹LSCE/IPSL, Laboratoire des Sciences du Climat et de l'Environnement, CEA-CNRS-UVSQ, Gif-sur-Yvette, France

²LMD (Laboratoire de Météorologie Dynamique), Palaiseau, France

³CNRM UMR 3589, Météo-France/CNRS, Toulouse, France

⁴LMD (Laboratoire de Météorologie Dynamique), IPSL, CNRS-ENS-UPMC-X, Département de Géosciences, École Normale Supérieure, Paris, France

*Now at: Department of Earth, Ocean and Ecological Sciences, School of Environmental Sciences, University of Liverpool, Liverpool L69 3GP, UK

Correspondence to: Camille Richon (crichon@liverpool.ac.uk)

Abstract. The Mediterranean region is a climate change hot-spot. Increasing greenhouse gas emissions are projected to lead to a significant warming of Mediterranean Sea waters, as well as major changes in its circulation, but the subsequent effects of such changes on marine biogeochemistry are still poorly understood. Our aim is to investigate the changes in nutrient concentrations and biological productivity in response to climate change in the Mediterranean region. To do so, we perform transient simulations with the coupled high resolution model NEMOMED8/PISCES using the pessimistic IPCC SRES-A2 socio-economic scenario and corresponding Atlantic, Black Sea, and coastal nutrient inputs. Our results indicate that nitrate is accumulating in the Mediterranean Sea over the 21st century, whereas no tendency is found for phosphorus. These contrasted variations result from an unbalanced nitrogen-to-phosphorus input from external sources and lead to changes in phytoplankton nutrient limitation factors. In addition, phytoplankton net primary productivity is reduced by 10 % in the 2090s in comparison to the present state, with reductions of up to 50 % in some regions such as the Aegean Sea as a result of nutrient limitation and vertical stratification. We also perform sensitivity tests in order to study separately the effects of climate and biogeochemical input changes on the Mediterranean future state. This article is a first step in the study of transient climate change effects on the Mediterranean biogeochemistry, but calls for coordinated multi-model efforts to explore the various uncertainty sources of such a future projection.

1 Introduction

The Mediterranean basin is enclosed by three continents, with mountains, deserts, rivers, and industrialized cities. This area is known as one of the most oligotrophic marine environment in the world



(Béthoux et al., 1998). Because of its high anthropogenic pressure and low biological productivity, this region is predicted to be highly sensitive to future climate change impacts (Giorgi, 2006; Giorgi and Lionello, 2008).

Records of the past evolution of the Mediterranean circulation show that the Mediterranean has undergone abrupt changes in its circulation patterns over ancient times. In particular, high stratification events, characterized by the preservation of organic matter in the sediment, known as sapropels, have been recorded through the last 10 000 years. This accumulation of organic matter in the sediments is interpreted as the result of a strong stratification of the water column leading to suboxic deep layers (e.g. Rossignol-Strick et al., 1982; Rohling, 1991, 1994; Vadsaria et al., 2017). In more recent times, abnormal winter conditions have led to changes in deep water formation, such as the Eastern Mediterranean Transient (EMT) event that occurred during the early nineties (see Theoharis et al., 1999; Lascaratos et al., 1999; Nittis et al., 2003; Velaoras and Lascaratos, 2010; Roether et al., 2014) and had biogeochemical impacts. Also, changes in the North Ionian Gyre circulation triggered the so-called Bimodal Oscillating System (BiOS) that influences phytoplankton bloom in the Ionian Sea (Civitaresi et al., 2010). The modification of water transport led to modified nutrient distribution that can alter local productivity. These events show that a semi-enclosed basin with short residence time of water such as the Mediterranean is highly sensitive to climate conditions and that changes in these conditions can trigger important circulation changes, ultimately leading to changes in the biogeochemistry.

The Mediterranean is connected to the global ocean by the narrow Strait of Gibraltar through which transport contributes substantially to its water and nutrient budgets (e.g. Gómez, 2003; Huertas et al., 2012). Future climate projections yield an increase in temperature and a decrease in precipitation over the Mediterranean region (Giorgi, 2006; IPCC, 2012) leading to warmer and saltier seawater (Somot et al., 2006; Adloff et al., 2015). As a result of these changes, the Mediterranean thermohaline circulation (MTHC) may significantly change with a consistent weakening in the western basin for greenhouse gases high-emission scenarios and a less certain response in the eastern basin (Somot et al., 2006; Adloff et al., 2015). In one of these MTHC weakening scenarios, Herrmann et al. (2014) show, in addition, a vertical stratification increase (Adloff et al., 2015). This will likely lead to weaken the vertical mixing that finally may reduce nutrient supply in the upper layer of the Mediterranean that is essential for phytoplankton to bloom (d'Ortenzio and Ribera d'Alcalà, 2009; Herrmann et al., 2013; Auger et al., 2014).

Primary productivity in the ocean is influenced by water circulation and vertical mixing that bring together available nutrients and phytoplankton (Harley et al., 2006). Changes in oceanic physics such as modification of vertical mixing can have dramatic effects on plankton community dynamics and ultimately on the productivity of the entire oceanic food web (Klein et al., 2003; Civitaresi et al., 2010). Few studies have investigated the sensitivity of the oligotrophic Mediterranean Sea to future climate change (e.g. Herrmann et al., 2014, for the northwestern Mediterranean). Lazzari et al.



(2014) investigated the effects of the A1B SRES (Special Report on Emissions Scenarios) moderate climate change scenario on the Mediterranean biological productivity and plankton communities. They performed short (10–year) non–transient simulations at the beginning and the end of the 21st century and found a decreasing trend of phytoplankton biomass in response to this climate change scenario. Macias et al. (2015) simulated a "baseline" of expected consequences of climate change alone on the Mediterranean primary productivity. They found that according to the RCP 4.5 and RCP 8.5 scenarios, integrated primary productivity over the eastern Mediterranean basin may increase as a result of density changes. However, their results are based on non–transient simulations and present–day nutrient inputs and the response of the Mediterranean biogeochemistry to transient climate and biogeochemical change scenarios has never been evaluated.

Being a semi–enclosed oligotrophic basin, the Mediterranean is highly sensitive to external nutrient inputs. Their origins are mainly from coastal runoff, river discharge (Ludwig et al., 2009), Atlantic inputs through Gibraltar (Gómez, 2003), and atmospheric deposition (Richon et al., 2017, 2018). This study aims at understanding the biogeochemical response of the Mediterranean to a "business–as–usual" climate change scenario throughout the 21st century. For this purpose, we use the high resolution coupled physical–biogeochemical model NEMOMED8/PISCES. We model the evolution of biogeochemical tracers (nutrients, chlorophyll–a concentrations, plankton biomass and primary production) under the SRES A2 climate change scenario for the 21st century (IPCC and Working Group III, 2000). The choice of the A2 scenario was driven by the availability of daily 3–D forcings for the biogeochemical model (Adloff et al., 2015). We are aware that using a single simulation will limit the robustness of our results. However the computer power required to perform large ensembles with PISCES and the unavailability of 3–D daily ocean transient scenario data currently prevent a more extensive assessment.

This article is organized as follows: the coupled model, forcings and the different simulations are first described. We briefly evaluate the biogeochemical model in Section 3.1 and present the evolution of the physical and biogeochemical forcings in Section 3.2. In section 3.3, we expose the temporal evolution of the main nutrients, their budgets in present and future conditions and discuss their impact on the biogeochemistry of the Mediterranean Sea.

2 Methods

2.1 The ocean model

The oceanic general circulation model used in this study is NEMO (Madec, 2008) in its regional configuration for the Mediterranean Sea (NEMOMED8 Beuvier et al., 2010). The NEMOMED8 grid has a horizontal resolution of $1/8^\circ$ stretched in latitude i.e., with a resolution from 9 km in the North to 12 km in the South of the domain. The model has 43 vertical levels with varying thicknesses (from 6 m in the surface layer to 200 m in the deepest layer). The Atlantic boundary is closed



at 11°W and tracers are introduced in a buffer zone between 11°W and 6°W.

Air–sea fluxes (momentum, heat, water) and river discharges used to force NEMOMED8 are pre-
95 scribed by the atmospheric Regional Climate Model ARPEGE–Climate (Déqué et al., 1994; Gibelin
and Déqué, 2003) using a global and stretched grid, which has a 50–km horizontal resolution over
the area of interest.

2.2 The SRES–A2 scenario simulation

ARPEGE–Climate is itself driven by greenhouse gases (GHG) and aerosol forcings following the
100 observations (up to year 2000) and the SRES–A2 scenario afterwards and by SST coming from a
previously run CNRM–CM coupled GCM (General Circulation Model) simulation (Royer et al.,
2002). In addition, the ocean component of CNRM–CM (a low resolution NEMO version) provides
the near–Atlantic conditions (3–D potential temperature and salinity) for NEMOMED8. The various
forcings and the modeling chain from the GCM to the ocean regional model are described in details
105 in Somot et al. (2006) and Adloff et al. (2015).

The NEMOMED8 simulation (ocean physics and forcings) used here corresponds to one of the
simulations used and studied in Adloff et al. (2015), and more specifically the simulations labeled
HIS (historical period 1961 to 1999) and A2 (A2 scenario period 2000–2099) in their Table 1.
This physical run has already been used to study climate change impacts on Mediterranean marine
110 ecosystems (Jordà et al., 2012; Hattab et al., 2014; Albouy et al., 2015; Andreello et al., 2015).

The main changes on the Mediterranean Sea physics (SST, SSS, surface circulation, deep convection
and thermohaline circulation, vertical stratification, sea level) that are detailed in Adloff et al. (2015).
Briefly, changes in temperature and precipitation in the A2 scenario lead to increased evaporation in
the basin. Freshwater inputs from rivers and the Black Sea decrease along with total precipitation.
115 This consequently leads to a significant increase in Gibraltar net transport (+0.018 Sv). Temperature
and salinity increase strongly, leading to a decrease in surface density and an overall increase in
vertical stratification. Average sea surface temperature of the Mediterranean rises by up to 3 K by
the end of the century. However, the temperature rise is not homogeneous in the basin, regions such
as the Balearic, Aegean, Levantine and North Ionian undergo a more intense warming (over 3.4 K)
120 probably due to the addition of the atmosphere-originated quasi-homogeneous warming with the
local effect of surface current changes. The salinity increases by 0.5 (practical salinity scale) on
average across the basin.

In the A2 simulation, the entire Mediterranean basin is projected to become more stratified by 2100
and deep water formation is generally reduced. These variations in hydrological characteristics of the
125 water masses generate important changes in the circulation and in particular in the vertical mixing
intensity. The strong reduction in vertical mixing observed in all deep water formation areas of the
basin is linked with the changes in salinity and temperature of the water masses. Reduced vertical



mixing may also reduce nutrient supply to the surface waters. A reduction in deep convection may also tend to reduce the loss of P and N to the sediment.

130 2.3 The biogeochemical model

Here, the physical model NEMOMED8 is coupled to the biogeochemical model PISCES (Aumont and Bopp, 2006), already used for investigations in the Mediterranean basin (Richon et al., 2017, 2018). This Monod-type model (Monod, 1958) has 24 biogeochemical compartments including 2 phytoplankton (nanophytoplankton and diatoms) and 2 zooplankton size classes (microzooplankton
135 and mesozooplankton). Phytoplankton growth is limited by the external concentration of five different nutrients: nitrate, ammonium, phosphate, silicic acid and iron. In this version of PISCES, elemental ratios of C:N:P in the organic matter are fixed to 122:16:1 following Takahashi et al. (1985). The biogeochemical model is ran in offline mode (see e.g. Palmieri et al., 2015): biogeochemical quantities are passive tracers, they are transported following an advection-diffusion equation using
140 dynamical fields (velocities, mixing coefficients...) calculated beforehand in a separate simulation with only the dynamical model NEMOMED8.

2.4 Boundary and initial physical and biogeochemical conditions

External nutrient supply for the biogeochemical model include inputs from the Atlantic Ocean and from Mediterranean rivers. Atlantic input is prescribed from water exchange at the Strait of Gibraltar
145 in the NEMO circulation model along with the concentrations of biogeochemical tracers in the buffer zone. Nutrient concentrations in the buffer zone are prescribed from a global ocean climate projection using the A2 simulation values from IPSL-CM5-LR (Dufresne et al., 2013) performed within the framework of the CMIP5 project (Taylor et al., 2012). Nutrient concentrations in the buffer-zone are relaxed to these values with a time constant of one month.

150 Nutrients input from rivers are derived from Ludwig et al. (2009) before 2000. For the 21st century, we use the estimations for nutrient discharge proposed by Ludwig et al. (2010) of the "Business As Usual" scenario from the Millenium Ecosystem Assessment (MEA) (Cork et al., 2005), which gives nitrate and phosphate discharge per sub-basin in 2030 and 2050. Yearly values are obtained by linear interpolation between 2000 and 2030 and between 2030 and 2050, after which they are held constant
155 until the end of the simulation in 2100. Seasonal variability coming from the four largest rivers for Mediterranean and Black Sea (Rhône, Po, Ebro and Danube) is also included. According to Ludwig et al. (2010), the future trends in nutrient discharge from the major rivers of the Mediterranean stay within the interannual variability over the past 40 years. However, if the riverine nutrient input is not drastically changed at the basin scale, Ludwig et al. (2010) point out some substantial changes in the
160 nutrient and water budget in specific regions. In particular, according to their scenario, the northern part of the Mediterranean has decreasing trends in nitrate discharge whereas it is increasing in the southeastern Levantine. Freshwater discharge from Ludwig et al. (2010) is based on the SESAME



model reconstruction and differs from the ARPEGE–Climate model used here. This may lead to incoherencies between water and nutrient discharges but the nutrient discharges from Ludwig et al. (2010) are the only available values, and the SESAME model is not coupled with NEMO/PISCES. Initial nutrient concentrations in the Mediterranean come from the SeaDataNet database (Schaap and Lowry, 2010) and initial nutrient concentrations in the buffer zone are prescribed from the World Ocean Atlas (WOA) (Locarnini et al., 2006). Salinity and temperature are initialized from the MEDATLAS II climatology of Fichaut et al. (2003).

All simulations begin from a restart of a historical run starting in January 1965 following a spin-up of more than 115 years done with a loop of the period 1966 to 1981 for the physical forcings and the river nutrient discharge.

2.5 Simulation set-up

All simulations are performed for 120 years (from 1980 to 2100). The control run CTRL is performed with present-day conditions forcing (1966–1981). The scenario simulation is referred to as HIS/A2 as in Adloff et al. (2015). HIS is the name of the historical period (in our case between 1980 and 1999), and A2 is the name of the 2000–2099 scenario simulation.

In order to quantify separately the effects of climate and biogeochemical forcings, we performed 2 additional control simulations: CTRL_R with climatic and Atlantic conditions corresponding to present-day conditions and river nutrient discharge following the scenario evolution, and CTRL_RG with climatic conditions corresponding to present-day conditions, and river nutrient discharge and Atlantic buffer-zone concentrations following the scenario conditions. Table 1 describes the different simulations. The effects of external nutrient inputs independent of climate effect are derived by CTRL_R-CTRL and CTRL_RG-CTRL_R. Similarly, to derive the effects of climate change and nutrient input change on nutrient budgets, we use the difference between HIS/A2 and CTRL. To derive the effects of climate change only, we calculate the difference between HIS/A2 and CTRL_RG.

3 Results

3.1 Evaluation of the NEMOMED8/PISCES model

NEMOMED8 has already been used in a number of regional Mediterranean Sea modeling studies either in hindcast mode (Beuvier et al., 2010; Herrmann et al., 2010; Sevault et al., 2014; Soto-Navarro et al., 2015; Dunić et al., 2016) or scenario mode (Adloff et al., 2015). It produces the main characteristics of the Mediterranean Sea circulation. Evaluation of the HIS simulation provided in Adloff et al. (2015) shows that the main physical characteristics of the Mediterranean are produced, in spite of a too cold upper layer (1 K colder than observations) and too little stratification in comparison to observations. In particular, the HIS simulation matches closely the observed thermohaline circulation in the Adriatic and Ionian basins (see Adloff et al., 2015).



The regional NEMOMED physical model has already been coupled to the biogeochemical model PISCES on a $1/12^\circ$ grid horizontal resolution (Palmieri et al., 2015; Richon et al., 2017, 2018), but no future climate simulation has yet been performed. As a first study coupling NEMOMED8
200 with PISCES, we compared the main biogeochemical features of our control simulation with available data. Figure 1 shows the surface average chlorophyll concentrations in the top 10 meters of the CTRL and HIS simulations, and from satellites estimations. The model correctly reproduces the main high-chlorophyll regions such as the Gulf of Lions and coastal areas. The west-to-east gradient of productivity is also reproduced by the model with values that agree with satellite estimates.
205 Moreover, this Figure shows that chlorophyll produced by the CTRL is stable over time. The model fails, however, to reproduce the observed chlorophyll-rich areas in the Gulf of Gabes and at the mouth of the Nile. Even though the satellite estimates are uncertain in the coastal areas, the model seems to underestimate chlorophyll concentrations in those regions. This discrepancy is probably linked with insufficient simulated nutrient discharge from coastal runoff in these regions.
210 The vertical distribution of nitrate and phosphate over a section crossing the Mediterranean from East to West as well as chlorophyll concentration profiles at the DYFAMED station are shown in appendix (Figures A1 and A2). In spite of some underestimation of nutrient concentrations that are probably linked with the features of the simulated intermediate and deep waters characteristics, the PISCES model reproduces the main characteristics of the Mediterranean biogeochemistry, including
215 a salient west-to-east gradient in nutrient concentrations, low surface nutrient concentrations and a deep chlorophyll maximum (DCM). The average chlorophyll concentration observed at the DYFAMED station in the top 200 m is $227 \pm 136 \text{ } 10^{-9} \text{ g L}^{-1}$ (average over the 1991–2005 period), while the model value for the HIS period is $173 \pm 150 \text{ } 10^{-9} \text{ g L}^{-1}$. These performances lend credence to our efforts to investigate the evolution of the Mediterranean biogeochemistry under the A2
220 climate change scenario with the same modeling platform.

3.2 Evolution of temperature and salinity

Average surface temperature and salinity (SST and SSS) evolution in the entire basin during the CTRL and HIS/A2 simulations are shown in Figure 2, which confirms results from Adloff et al. (2015) and shows that the CTRL simulation is stable over time. Beyond this global average variation
225 in SST and SSS, a more detailed analysis reveals much greater variability depending on the region (Somot et al., 2006; Adloff et al., 2015).

3.3 Evolution of the nutrient budgets in the Mediterranean Sea

The nutrient budgets of the semi-enclosed Mediterranean basin are highly dependent on external
230 sources. In order to map the effects of climate change on the Mediterranean nutrient balance, we calculated mass budgets of nitrate and phosphate during the simulated period. These budgets take into



account changes in Atlantic input, river discharge and sedimentation. Nitrate can also accumulate in the Mediterranean waters through N_2 fixation by cyanobacteria, but this process accounts for less than 1 % of the total nitrate budget (Ibello et al., 2010; Bonnet et al., 2011; Yogeve et al., 2011), and is neglected here.

In this Section, we refer to the period 1980–1999 as the beginning of the century, to the period 2030–2049 as the middle of the century and to the period 2080–2099 as the end of the century. Also, we derive the effects of river input changes as the difference of nutrient concentrations between CTRL_R and CTRL over these time periods. Similarly, the effects of changes in Gibraltar exchange are derived by the differences between CTRL_RG and CTRL_R, and the effects of climate change by the difference between HIS/A2 and CTRL_RG.

3.3.1 Evolution of phosphate and nitrate concentrations

In order to observe the general evolution of tracer concentrations over the 21st century, we plotted the evolution of the main limiting nutrients (phosphate and nitrate) concentrations for the entire simulation period in the western and eastern basins. The separation between western and eastern basin is the Sicily Strait. Therefore, the eastern basin includes the Ionian, Levantine, Adriatic and Aegean basins. Figure 3 shows the evolution of average phosphate concentrations in the western and eastern basin, respectively, for the surface (0–200 m), intermediate (200–600 m) and bottom (> 600 m) layers of the water column.

We observe that phosphate concentration in HIS/A2 decreases in the surface and intermediate layers of the western basin until the middle of the century and then increases again until the end of the century. Figure 3a shows that phosphate concentrations in the CTRL_RG simulation differ significantly from those in CTRL at the end of the 21st century. This is a sign that phosphate concentration in the western basin is strongly linked to Gibraltar inputs. However, the concentrations in the CTRL_RG simulation do not differ significantly from the CTRL simulation in the intermediate layer (Figure 3b). Nutrients enter the Mediterranean at Gibraltar through the surface layer and leave through intermediate and deep waters. A slight accumulation of phosphate is observed in the deep western basin. The significant difference between the HIS/A2 simulation and the control runs shows that the evolution of the Mediterranean physics linked with climate change is primarily responsible for the changes in phosphate concentration in the intermediate and deep western basin.

The eastern part of the basin contains approximately 50 % less phosphate than the western part. In the surface layer, phosphate concentration decreases in the beginning of the simulation and remain low during the 21st century (Figure 3d). We observe in Figures 3e and 3f a slight accumulation of phosphate in the intermediate and deep layers and large decennial variability of phosphate concentration in the deep eastern basin.



The evolution of nitrate concentration shows a marked accumulation over the century in all regions of the intermediate and deep Mediterranean waters (Figures 4b, 4c, 4e and 4f). In the surface waters
270 of the western basin, nitrate concentrations are stable until the middle of the 21st century, and then sharply increase until the end of the simulation period. This evolution follows nitrate inputs from the Atlantic. Nutrient dynamics in the surface western basin seem mainly dependent on Gibraltar exchanges.

In the eastern basin, the impacts of river discharges of nitrate seem to have large influence on the ni-
275 trate accumulation as shown by the similar evolution of HIS/A2 and CTRL_R simulations. However, the evolution of physical conditions seems to have similarly large impacts on the nitrate concentrations in the eastern basin as shown by the difference between CTRL_R and HIS/A2.

The large differences between the CTRL simulations and the HIS/A2 shows that modification of circulation resulting from climate change have substantial impacts on the deep and intermediate nu-
280 trient concentrations. Figure 4d shows the contrasted effects of climate and biogeochemical changes. The strong difference between CTRL_R and CTRL concentrations at the beginning of the simulation indicates that riverine nutrient discharge has a strong influence on surface nitrate concentrations in the eastern basin. But the strong difference between CTRL_R and HIS/A2 at the end of the century indicates that vertical stratification leads to a decrease in surface layer nitrate concentrations,
285 probably linked with nutrient exhaustion. In the intermediate and deep layers of the eastern basin (Figures 4e and 4f), nitrate concentrations increase as a result of the effects of both climate and river discharge changes. In contrast, the difference between HIS/A2 and CTRL_RG phosphate concentrations (Figure 3) indicates that the variations of phosphate concentrations during the 21st century are primarily linked with climate change.

290 3.3.2 Exchange fluxes of nutrients at Gibraltar

The Mediterranean is a remineralization basin that has net negative fluxes of inorganic nutrients (i.e. organic nutrients enter the basin through the Gibraltar Strait surface waters and inorganic nutrient leave the Mediterranean through the deep waters of the Gibraltar Strait Huertas et al., 2012). We observe similar trends in phosphate and nitrate fluxes linked to the Redfieldian behavior of the primary
295 production in PISCES. According to the HIS/A2 simulation, the incoming fluxes decrease slightly until the middle of the century and then increase to reach values higher than the control in the last 25 years of simulations (Figure 5). Outgoing fluxes follow the same trends as incoming fluxes. We observe a drift in the nitrate outgoing flux in the control. At the end of the 21st century, incoming fluxes of nutrient have increased in the scenario simulation by about 13 % (difference between the
300 2080–2099 and 1980–1999 periods). But this significant increase follows a decrease of over 20 % in incoming nutrient fluxes between the 1980–1999 and the 2030–2049 periods. Outgoing fluxes increase less between the beginning and the end of the century (3.5 and 3.9 % for phosphate and nitrate respectively, Figure 5). These trends result from the evolution of water fluxes through the Strait



of Gibraltar computed by NEMOMED8 and the A2 scenario of nutrient concentrations in the buffer
305 zone taken from Dufresne et al. (2013). Figures 3a and 5b show that the evolution of phosphate
concentration in the western basin is linked with Gibraltar inputs (Pearson's correlation coefficient
is 0.63, p -value= 10^{-14}).

The imbalance between incoming and outgoing nutrient flux anomalies may be a cause for the ob-
served accumulation of inorganic nutrients (in particular of nitrate) in the basin.

310 3.3.3 River fluxes of nutrients

River discharge is the main external source of nutrient for the eastern part of the basin. Figure 6
shows the total river discharges to the Mediterranean Sea in nitrate and phosphate during the simu-
lation period.

315 Nitrate discharge in the HIS/A2 simulation is significantly higher than in CTRL. nitrate total dis-
charge in the Mediterranean has continuously increased from the 1960s (see the CTRL values for
the years 1966–1981). According to the HIS/A2 simulation, total river nitrate discharge is 24 %
larger during 2080–2099 than during 1980–1999. Simultaneously, phosphate discharge decreases by
25 %. As suggested by Ludwig et al. (2010), phosphate discharge in the A2 period stays lower than
320 in the HIS period, in spite of a small discharge enhancement between 2030 and 2049.

3.3.4 Sedimentation

Sedimentation removes nutrients from the Mediterranean Sea. In this version of PISCES, the loss of
nitrogen and phosphorus to the sediment is calculated from the sinking of organic carbon particles to
the sediment (linked through the Redfield ratio). Sediment fluxes of phosphorus and nitrogen during
325 the simulations are shown in Figure 7.

The loss to the sediment decreases rapidly during the HIS simulation (1980–1999). By the end
of the 21st century, sedimentation of P and N are almost 50 % lower relative to the 1980 fluxes. This
strong decrease in sedimentation that occurs despite an enhancement in nutrient flux coming from
330 the Atlantic and an enhanced nitrate river flux may be linked to the decrease in vertical water fluxes,
which would explain the accumulation of phosphate and nitrate in the deep layers of the Mediter-
ranean Sea (Figures 3c, 3f, 4c and 4f).

In general, the sum of nitrogen fluxes in the Mediterranean basin increases by 39 % at the end
335 of the century in the scenario (HIS/A2) whereas it is increased by 23 % in the control (CTRL). The
sum of phosphorus fluxes increases by 9 % in the scenario and by 11 % in the control. These results
suggest a significant accumulation of nitrogen in the Mediterranean basin over the century when
phosphorus fluxes can be considered roughly stable.



340 Tables 2 and 3 summarize the average phosphate and nitrate content in all simulations for 3 periods of time: the beginning of the century (1980–1999), the middle of the century (2030–2049) and the end of the century (2080–2099).

345 Phosphate content in the entire Mediterranean has increased in our simulation by 6 % over the 21st century, as determined by the difference between CTRL and HIS/A2 simulations between 1980–1999 and 2080–2099. The increase is more important in the eastern basin than in the western basin. In particular, we observe an 8 % increase in phosphate content in the Ionian–Levantine sub-basin in 2080–2099 compared to 1980–1999. The effects of phosphate river input changes are substantial over the first half of the century. We observe 3 % decrease in phosphate content in the entire Mediterranean between 1980–1999 and 2030–2049 due to river input changes (difference between CTRL_R and CTRL). Changes in Gibraltar exchange fluxes of phosphate seem to have limited effect on the Mediterranean phosphate content. However, climate change effects lead to a global enhancement of 10 % in phosphate content in 2080–2099 in comparison to 1980–1999. This result shows contrasted effects of physical and biogeochemical conditions on the evolution of nutrient concentrations. Climate change effects lead to an accumulation of phosphate that is probably linked to a decrease in primary productivity (hence, in nutrient consumption), decreased sediment fluxes (see Figure 7), and increased stratification, thus isolating most of the phosphate pool from the surface.

365 Table 3 shows that in the model, the combined effects of climate, riverine and Atlantic nutrients input changes over the 21st century lead to a 17 % increase in nitrate content over the Mediterranean in the 2080–2099 period compared to 1980–1999 (derived from the calculation of HIS/A2–CTRL). Changes in river discharge in the Mediterranean over the century lead to 9 % enhancement of nitrate content by the end of the century (2080–2099) compared to the beginning of the simulation period (1980–1999). The most important effects of river input changes are observed in the Adriatic basin (over 50 % nitrate accumulation by the end of the century). Over the entire Mediterranean, the effects of Gibraltar input changes on nitrate content are weak (< 1 %). However, the comparison of nitrate content in CTRL_R and CTRL_RG in the western basin shows a 3 % decrease in nitrate content in the western basin during the 2030–2049 period followed by an increase resulting in +1 % nitrate by 2080–2099 compared to the 1980–1999 period. Finally, climate change effects lead to 7 % increase in nitrate content over the Mediterranean basin in the 2080–2099 period compared to 1980–1999 (computed by HIS/A2–CTRL_RG). These results indicate that river inputs and climate change are the main drivers of nitrate content changes in the Mediterranean basin over the 21st century.



3.4 Present and future biological productivity and nutrient limitations in the surface Mediterranean

Figures 8 and 9 show the average surface concentrations of nitrate and phosphate in the beginning of the century (1980–1999) and the end of the century (2080–2099) in the HIS/A2 and CTRL simulations. In the Mediterranean Sea, biological productivity is mainly limited by these 2 nutrients and their evolution in the future may determine the productivity of the basin. Figure 8 confirms the previous results and shows an accumulation of nitrate in large zones of the basin, except for the southwestern part of the western basin (Alboran Sea) and a small area in the southeastern Levantine that appears to be the result of Nile discharge influence.

On the contrary, Figure 9 shows that phosphate surface concentration is decreasing everywhere in the basin except near the mouth of the Nile and in the Alboran Sea. The specific concentrations observed next to the Nile mouth are linked with an inversion of the N:P ratio (i.e. increase in P discharge and decrease in N discharge) in this river in our scenario. The distribution of surface phosphate at the end of the century (2080–2099) shows that all P-rich areas of the eastern basin at the beginning of our simulations are largely depleted by the end of the simulation. For instance, the P rich area between Crete and Cyprus is no longer observed in the 2080–2099 period (Figure 9). Moreover, Figure 10 shows that this area matches a productive zone observed in the 1980–1999 period. All the most productive zones of the beginning of the century are reduced in size and intensity by the end of the century. The primary production integrated over the euphotic layer (0–200 m) is reduced in our simulation by 10 % on average between 1980–1999 and 2080–2099. However, Figure 10 shows a productivity decrease of more than 50 % in areas such as the Aegean Sea and the Levantine Sea. In general, the differences in surface biogeochemistry between the 1980–1999 and 2080–2099 periods are weaker in the western basin because of the strong regulating impact of Gibraltar nutrient exchange.

We also observe local changes in nutrient concentrations and primary production. For instance, around Majorca Island, Corsica and Cyprus, changes in local concentrations of nutrients have substantial effects on primary productivity. These mesoscale changes may be linked with local circulation changes (such as mesoscale eddies). These observations show that the evolution of the Mediterranean biogeochemistry is influenced by both meso and large scale circulations patterns.

Figure 11 presents the limiting nutrient calculated using PISCES half-saturation coefficients (see Aumont and Bopp, 2006). The limiting nutrient is derived from the minimal value of limitation factors. In the Monod-type model PISCES, nutrient-based growth rates follow a Michaëlis–Menten evolution with nutrient concentrations. In the present period, most of the productive areas are N and P colimited in the simulation (Figure 11). This includes regions such as the Gulf of Lions, the South Adriatic, the Aegean Sea and the northern Levantine. Future accumulation of nitrogen in the basin would modify the nutrient balance causing most eastern Mediterranean surface waters to become P-



limited. Thus, future phosphate surface concentrations in the Mediterranean would tend to decrease.

410 The total balance of phosphate is more negative in the future than in the present period whereas we observe an inverse situation for nitrate. Therefore, phosphate would become the major limiting nutrient in most of the regions where productivity is reduced such as the Aegean Sea, the northern Levantine basin and the South Adriatic.

415 3.5 Modifications of the Mediterranean deep chlorophyll maximum

One specificity of Mediterranean biology is that most planktonic productivity occurs below the surface at a depth called the deep chlorophyll maximum (DCM). Hence, most of the chlorophyll concentration is not visible by satellites (Moutin et al., 2012). Figure 12 shows the average depth of the simulated DCM for the period 1980–1999 and for the period 2080–2099.

420

We observe that the DCM depth changes little during the simulation, even though the physical characteristics of the water masses do change. The DCM tends to deepen slightly in some regions such as the South Ionian and the Tyrrhenian basin. These results suggest that the DCM depth is not significantly altered in the future but the intensity of subsurface productivity seems reduced (see Figure 10).

425

Figure 13 shows the average vertical profiles of chlorophyll at the DYFAMED station (43.25° N, 7.52° E) and the average profiles for the western and eastern basins for the 1980–1999 and 2080–2099 periods. The results show that the subsurface chlorophyll maximum is still modeled at the end of the century. At the DYFAMED station, the average DCM depth is unchanged but surface concentration is reduced. However, we simulated seasonal variability in the chlorophyll concentration profiles at the station with intensity and depth of DCM reduced by about 40 % for some month (not shown). In the western basin, the subsurface maximum in the present and future periods is located at the same depth (100–120 m), but the average productivity is reduced by almost 50 %, which confirms the results from Figure 12. In the eastern basin, it is reduced and the subsurface productivity maximum deepens from 100–120 m to below 150 m.

435

In the oligotrophic Mediterranean, the majority of the chlorophyll is produced within the DCM. The changes in DCM we observe combined with external nutrient input changes result in 17 % reduction in integrated chlorophyll production between the 1980–1999 and 2080–2099 periods. Table 4 reports total chlorophyll production in the 1980–1999, 2030–2049 and 2080–2099 periods of all the simulations in all Mediterranean subbasins Adloff et al. (Figure 2 2015). Table 4 shows that chlorophyll production is stable over the CTRL simulation but decreases in all Mediterranean subbasins over the HIS/A2 simulation. The decrease in chlorophyll production is more important in the eastern regions, in particular in the Adriatic and Aegean Seas (-29 and -15 % respectively). In the

440



445 western basin, the loss of chlorophyll is smaller (-13 %). The chlorophyll production is probably
maintained by the enhancement of Gibraltar nutrient fluxes (chlorophyll production in CTRL_RG
does not significantly decrease in the western basin).

The results indicate that 85 % of the reduction in chlorophyll production in the future period mod-
450 eled in the HIS/A2 simulation is explained by climate effects (difference between HIS/A2 and
CTRL_RG). However, the effects of increased Gibraltar inputs, decreased riverine phosphate in-
puts and increased nitrate inputs seem to have opposing effects to climate and circulation changes
on chlorophyll production. In particular, in the western basin, changes in riverine discharge of nu-
trients seem to reduce chlorophyll production (see CTRL_R values), whereas changes in Gibraltar
455 inputs seem to enhance chlorophyll production (see CTRL_RG).

3.6 Plankton biomass evolution

Most of the biological activity in the marine environment is confined to the euphotic layer which
is confined to the upper 200 m. Figure 14 shows the evolution of nanophytoplankton and diatom
concentrations in the top 200 m for the entire simulation period in all simulations in the western and
460 eastern basins. We observe for both phytoplankton classes their biomass across the Mediterranean
Sea are lower at the end of the century than in the present conditions. In general, diatoms seem
more sensitive to climate change and their biomass decreases more sharply than nanophytoplankton.
Moreover, Figure 14c shows that diatom concentrations seem to be sensitive to changes in nutri-
ent input across the Strait of Gibraltar as indicated by the large difference between CTRL_RG and
465 CTRL_R. However, the low concentration observed in HIS/A2 indicates that the evolution of the
diatom concentration over the 21st century is primarily influenced by climatic drivers.

Figure 15 shows the evolution of zooplankton biomass in the top 200 m during the simulation.
The same general evolution is found for the simulated phytoplankton: a decrease in microzooplank-
470 ton during 1980–2000, after which it remains stable until the end of the simulation in 2100. in all
basins; a large drawdown in mesozooplankton levels in the eastern basin. The average mesozoo-
plankton concentration in the eastern part of the Mediterranean declines by almost 60 % in 2099
in comparison to 1980. In the western basin, we observe a marked decrease of mesozooplankton
concentrations between 1980 and 2040. After 2040, surface concentrations of mesozooplankton in-
475 creases regularly to similar values than at the beginning of the simulation. This evolution is similar
to those for nutrient concentrations in surface waters of the western basin (Figure 3). In the PISCES
model, zooplankton, and in particular mesozooplankton is highly sensitive to the variations of ex-
ternal climatic and biogeochemical conditions because that is the highest trophic level represented.
Owing to their bottom–up control, zooplankton canalize all changes at the basin scale and ultimately
480 displays the largest response. This behavior is similar to the trophic amplification observed by Chust



et al. (2014) and Lefort et al. (2015).

After all, the analysis of plankton biomass evolution during the simulation period suggests that primary and secondary production in the eastern basin are more sensitive to climate change than
485 the western basin in this simulation. The eastern part of the basin is more isolated from the open
Atlantic Ocean than is the western part and it receives less nutrients from the Atlantic and from
coastal inputs. The eastern basin is also deeper and less productive than the western basin (Crispi
et al., 2001). The eastern basin exhibits a decline in the phytoplankton biomass that is similar to the
decline in the phosphate concentration. Biological production is mainly P-limited in this basin (see
490 also Figure 11). Therefore, the constant low concentrations of phosphate observed throughout this
century limit biological production and keep plankton biomass at low levels.

4 Discussion

4.1 Biogeochemical forcings

Climate change may impact all drivers of biogeochemical cycles in the ocean. In the case of semi-
495 enclosed seas like the Mediterranean, the biogeochemistry is primarily influenced by external sources
of nutrients (namely rivers, Atlantic and atmospheric inputs) and modification of the physical ocean
(vertical mixing, horizontal advection, ...). Nutrient fluxes from these sources may evolve separately
and differently depending on socioeconomic decisions and climate feedbacks. In this study, differ-
ent scenarios were used for river inputs ("Business as Usual" from Ludwig et al., 2010, based on the
500 Millennium Ecosystem Assessment report) and for Atlantic nutrient concentrations (SRES/A2 from
Dufresne et al., 2013). No atmospheric deposition was considered in this study because there is, to
our knowledge, no transient scenario for atmospheric deposition evolution over the Mediterranean
Sea. Scenarios from the MEA report are based on different assumptions from the IPCC SRES sce-
narios used to compute freshwater runoff in the HIS/A2 simulation. Moreover, the Ludwig et al.
505 (2010) nutrient discharge transient scenario does not represent the interannual variability of nutrient
runoff. Other studies by Herrmann et al. (2014) and Macias et al. (2015) used continued present-
day discharge of nutrients. As there is no consensus nor validated scenario for nutrient fluxes from
coastal runoff in the Mediterranean, we chose to use one scenario from Ludwig et al. (2010). This
scenario has the advantage of being derived from a coherent modeling framework. However, accord-
510 ing to these authors, the socio-economic decisions made in the 21st century will influence nitrate
and phosphate discharge over the Mediterranean. It is difficult to forecast these decisions and the
resulting changes in nutrient discharges are uncertain. Moreover, our results emphasize that the bio-
geochemistry in many coastal regions of the Mediterranean Sea such as the Adriatic Sea are highly
influenced by coastal nutrient inputs. In these regions, the effects of nutrient runoff changes seem
515 more important than climate change effects (see Table 4). Therefore, the choice of coastal runoff



scenario will greatly influence the results in these regions. Associated discrepancies and the uncertainties linked with the use of inconsistent scenarios in our simulation should be addressed by developing a more integrated modeling framework to study the impacts of climate change on the Mediterranean Sea biogeochemistry.

520 4.2 Climate change scenario

Although the physical model adequately represents the MHTC (Adloff et al., 2015), there are many uncertainties linked with climate change projections. Some are discussed in Somot et al. (2006), in particular, the need to using different IPCC scenarios for climate change projections and THC changes. Adloff et al. (2015) apply an ensemble of SRES scenarios and boundary conditions to
525 the Mediterranean Sea and discuss their effects on MTHC. In particular, their results suggests that the choice of atmospheric and Atlantic conditions has a strong influence on the MTHC. The A2 scenario that we used was the only available with 3-D daily forcings for coupling with the PISCES biogeochemical model. However, Adloff et al. (2015) showed that other SRES scenarios such as the A1B or B1 may lead to a future decrease in the vertical stratification with probably different
530 consequences on the Mediterranean Sea biogeochemistry. Our study should be considered as a first step for transient modeling of the Mediterranean Sea biogeochemistry but should be complemented by new simulations that explore the various sources of uncertainty (model choice, internal variability, scenario choice) once appropriate forcings become available for multiple models as expected from the Med-CORDEX initiative (Ruti et al., 2015).

535 4.3 Uncertainties from the PISCES model

The evaluation of the CTRL simulation showed that NEMOMED8/PISCES is stable over time in spite of a slight drift in nitrate concentrations (see Figure 4). Nutrient concentrations in the intermediate and deep layers were shown to be slightly underestimated in comparison to measurements (see appendix). Moreover, nitrate fluxes from coastal discharge in CTRL are lower than in HIS/A2.
540 This discrepancy and the imbalance in sources and sinks explains the loss of nitrate in the CTRL (see Figures 4 and 8). The simulated chlorophyll-a vertical profiles at the DYFAMED station show a correct representation of the subsurface productivity maximum of the Mediterranean in spite of a mismatch in the subsurface chlorophyll maximum depth between model and measurements. Model values were not corrected to match data, and we are therefore conscious that the uncertainties in
545 the representation of present-day biogeochemistry by the PISCES model may be propagated in the future.

In the PISCES version used in this study, nitrate and phosphate concentration variations are linked by the Redfield ratio (Redfield et al., 1963). The Redfield hypothesis of a fixed nutrient ratio used for plankton growth and excretion holds true for most parts of the global ocean, but may not be true
550 for oligotrophic regions such as the Mediterranean Sea (e.g. Béthoux and Copin-Montégut, 1986).



Moreover, changes in nutrient balance influence the nutrient limitations as shown by Figure 11. The results simulated with the Redfieldian hypothesis are coherent with the observed variations of nutrient supply to the Mediterranean Sea and yield realistic biological productivity. But results concerning nutrient limitations might change in a non Redfieldian biogeochemistry model.

555 4.4 Climate versus biogeochemical forcing effects

To our knowledge, this is the first attempt to study the basin-scale biogeochemical evolution using a transient business-as-usual (A2) climate change scenario. Lazzari et al. (2014) tested the effects of several land-use change scenarios on the A1B SRES climate change scenario over 10-years time slices. They found a general decrease in plankton biomass that is lower than in our severe climate change scenario. They also conclude that the river mouth regions are highly sensitive because the Mediterranean Sea is influenced by external nutrient inputs. Herrmann et al. (2014) studied the transient biogeochemical evolution of the northwestern Mediterranean Sea under the A2 and A1B scenarios with the coupled ECO3M-S/SYMPHONIE model. But they used present-day conditions for biogeochemical forcings, as did Macias et al. (2015). Results from Herrmann et al. (2014) indicate that chlorophyll production and plankton biomass increase slightly as a result of vertical stratification. Our results indicate that the contrasting effects of vertical stratification and changes in biogeochemical forcings may lead to a decrease in chlorophyll and plankton biomass production at the basin scale.

Results from our different control simulations indicates the extent to which the choice of the biogeochemical forcing scenario may influence the future evolution of the Mediterranean Sea biogeochemistry. In particular, nutrient inputs at Gibraltar have substantial consequences on the western basin. Moreover, climate and nutrient forcing changes may have contrasting influences on the Mediterranean Sea biogeochemistry. Stratification may lead to increased productivity in the surface because of the nutrient concentration increase (see also Macias et al., 2015), while decreasing coastal discharges of phosphate may decrease the productivity in the basin.

Conclusion

This study aims at assessing the transient effects on Mediterranean Sea biogeochemistry from climate and biogeochemical forcings under the IPCC A2 climate change scenario. The NEMOMED8/PISCES model adequately reproduces the main characteristics of the Mediterranean Sea: the west-to-east gradient of productivity, the main productive zones and the presence of a DCM, in spite of certain shortcomings. Hence it appears reasonable to use it to study the future evolution of the biogeochemistry of the Mediterranean basin in response to increasing atmospheric CO₂ and climate change. For the first time, we performed a continuous simulation over the entire period of the future IPCC scenario (A2), between 1980 and 2099.



585 This study illustrates how future changes in physical and biogeochemical conditions, including warming, increased stratification, and changes in Atlantic and river inputs, can lead to a significant accumulation of nitrate and a decrease in biological productivity in the surface, thus affecting the entire Mediterranean ecosystem.

Our results also illustrate how variations of the Mediterranean Sea biogeochemistry can be influenced by external nutrient inputs and that climate change and nutrient discharges have contrasted influences on the Mediterranean Sea productivity. In particular, the biogeochemistry in the western basin displays similar nutrient trends as does its input across the Strait of Gibraltar. Therefore, it appears critical to correctly represent the future variations of external biogeochemical forcings of the Mediterranean Sea as they may have equally important influence on biogeochemical cycles as climate. The eastern basin receives less nutrients from the Atlantic. As a consequence, its biogeochemistry is more sensitive to vertical mixing and river inputs and the stratification observed in the future leads to a steep reduction in surface productivity.

Finally, this study accounts for the changes in all external biogeochemical forcings except atmospheric deposition. However, Richon et al. (2017, 2018) showed that atmospheric deposition can account for up to 80 % of phosphate supply in some Mediterranean Sea regions and has significant impacts on surface productivity. We did not include atmospheric deposition in this study because there is to our knowledge no available transient scenario for 21st century evolution of atmospheric deposition. But this nutrient source may be subject to important changes in the future. A new generation of fully coupled regional models have been developed and used to study aerosols climatic impacts (Nabat et al., 2015). These models include a representation of the ocean, atmosphere, aerosols and rivers and should be used to perform future climate projections consistent at the Mediterranean regional scale.

Appendix A: Evaluation of the NEMOMED8/PISCES model

The comparison of modeled surface chlorophyll-*a* concentration with satellite estimates has revealed that the model correctly simulates the main characteristics observed in the Mediterranean Sea (Figure 1). Comparison with in situ observation provides more refined estimates.

Figure A1 presents the average chlorophyll-*a* profiles at the DYFAMED station (43.25°N, 7.52°E) compared with measured concentrations for the month of February (low stratification, high productivity) and June (high stratification, low productivity). There are few data points below 200 m. The model produces the characteristic of the deep chlorophyll maximum generated in June, even if its depth is too important.

The vertical distribution of nitrate and phosphate concentrations along a West-to-East transect is



620 showed in Figure A2. The model produces the salient West-to-East gradient of nutrient concentrations. Concentrations in the surface layer seem correct although the nutricline is too smooth, leading to the underestimated deep water concentrations.



References

- Adloff, F., Somot, S., Sevault, F., Jordà, G., Aznar, R., Déqué, M., Herrmann, M., Marcos, M., Dubois, C.,
625 Padorno, E., Alvarez-Fanjul, E., and Gomis, D.: Mediterranean Sea response to climate change in an ensemble of twenty first century scenarios, *Climate Dynamics*, 45, 2775–2802, doi:10.1007/s00382-015-2507-3, <http://link.springer.com/article/10.1007/s00382-015-2507-3>, 2015.
- Albouy, C., Leprieur, F., Le Loc'h, F., Mouquet, N., Meynard, C. N., Douzery, E. J. P., and Mouillot, D.:
630 Projected impacts of climate warming on the functional and phylogenetic components of coastal Mediterranean fish biodiversity, *Ecography*, 38, 681–689, doi:10.1111/ecog.01254, <http://doi.wiley.com/10.1111/ecog.01254>, 2015.
- Andreollo, M., Mouillot, D., Somot, S., Thuiller, W., and Manel, S.: Additive effects of climate change on connectivity between marine protected areas and larval supply to fished areas, *Diversity and Distributions*, 21, 139–150, doi:10.1111/ddi.12250, <http://onlinelibrary.wiley.com/doi/10.1111/ddi.12250/abstract>, 2015.
- 635 Auger, P. A., Ulses, C., Estournel, C., Stemmann, L., Somot, S., and Diaz, F.: Interannual control of plankton communities by deep winter mixing and prey/predator interactions in the NW Mediterranean: Results from a 30-year 3D modeling study, *Progress in Oceanography*, 124, 12–27, doi:10.1016/j.pocean.2014.04.004, <http://www.sciencedirect.com/science/article/pii/S007966114000524>, 2014.
- Aumont, O. and Bopp, L.: Globalizing results from ocean in situ iron fertilization studies: GLOBALIZING
640 IRON FERTILIZATION, *Global Biogeochemical Cycles*, 20, n/a–n/a, doi:10.1029/2005GB002591, <http://doi.wiley.com/10.1029/2005GB002591>, 2006.
- Beuvier, J., Sevault, F., Herrmann, M., Kontoyiannis, H., Ludwig, W., Rixen, M., Stanev, E., Béranger, K., and Somot, S.: Modeling the Mediterranean Sea interannual variability during 1961–2000: Focus on the Eastern Mediterranean Transient, *Journal of Geophysical Research: Oceans*, 115, C08 017,
645 doi:10.1029/2009JC005950, <http://onlinelibrary.wiley.com/doi/10.1029/2009JC005950/abstract>, 2010.
- Bonnet, S., Grosso, O., and Moutin, T.: Planktonic dinitrogen fixation along a longitudinal gradient across the Mediterranean Sea during the stratified period (BOUM cruise), *Biogeosciences*, 8, 2257–2267, doi:10.5194/bg-8-2257-2011, <http://www.biogeosciences.net/8/2257/2011/>, 2011.
- Béthoux, J. P. and Copin-Montégut, G.: Biological fixation of atmospheric nitrogen in the Mediterranean Sea, *Limnology and Oceanography*, 31, 1353–1358, doi:10.4319/lo.1986.31.6.1353, <http://onlinelibrary.wiley.com/doi/10.4319/lo.1986.31.6.1353/abstract>, 1986.
- 650 Béthoux, J. P., Morin, P., Chaumery, C., Connan, O., Gentili, B., and Ruiz-Pino, D.: Nutrients in the Mediterranean Sea, mass balance and statistical analysis of concentrations with respect to environmental change, *Marine Chemistry*, 63, 155–169, doi:10.1016/S0304-4203(98)00059-0, <http://www.sciencedirect.com/science/article/pii/S0304420398000590>, 1998.
- 655 Chust, G., Allen, J. I., Bopp, L., Schrum, C., Holt, J., Tsiaras, K., Zavatarelli, M., Chifflet, M., Cannaby, H., Dadou, I., Daewel, U., Wakelin, S. L., Machu, E., Pushpadas, D., Butenschon, M., Artioli, Y., Petihakis, G., Smith, C., Garçon, V., Goubanova, K., Le Vu, B., Fach, B. A., Salihoglu, B., Clementi, E., and Irigoien, X.: Biomass changes and trophic amplification of plankton in a warmer ocean, *Global Change Biology*, 20, 2124–2139, doi:10.1111/gcb.12562, <http://doi.wiley.com/10.1111/gcb.12562>, 2014.
- 660



- Civitaresse, G., Gacic, M., Lipizer, M., and Borzelli, G. L. E.: On the impact of the Bimodal Oscillating System (BiOS) on the biogeochemistry and biology of the Adriatic and Ionian Seas (Eastern Mediterranean), *Biogeosciences*, 7, 3987–3997, doi:10.5194/bg-7-3987-2010, wOS:000285574100006, 2010.
- Cork, S., Peterson, G., Petschel-Held, G., Alcamo, J., Alder, J., Bennett, E., Carr, E., Deane, D., Nelson, G., Ribeiro, T., and others: Four scenarios, Ecosystems and human well-being: Scenarios, 2, http://www.academia.edu/download/31005604/Millennium_assessment.pdf, 2005.
- 665 Crispi, G., Masetti, R., Solidoro, C., and Crise, A.: Nutrients cycling in Mediterranean basins: the role of the biological pump in the trophic regime, *Ecological Modelling*, 138, 101–114, doi:10.1016/S0304-3800(00)00396-3, <http://www.sciencedirect.com/science/article/pii/S0304380000003963>, 2001.
- 670 d’Ortenzio, F. and Ribera d’Alcalà, M.: On the trophic regimes of the Mediterranean Sea: a satellite analysis, *Biogeosciences*, 6, 139–148, <http://www.biogeosciences.net/6/139/2009/bg-6-139-2009.html>, 2009.
- Déqué, M., Dreveton, C., Braun, A., and Cariolle, D.: The ARPEGE/IFS atmosphere model: a contribution to the French community climate modelling, *Climate dynamics*, 10, 249–266, <http://cat.inist.fr/?aModele=afficheN&cpsid=4250659>, 1994.
- 675 Dufresne, J.-L., Foujols, M.-A., Denvil, S., Caubel, A., Marti, O., Aumont, O., Balkanski, Y., Bekki, S., Bellenlenger, H., Benshila, R., Bony, S., Bopp, L., Braconnot, P., Brockmann, P., Cadule, P., Cheruy, F., Codron, F., Cozic, A., Cugnet, D., Noblet, N. d., Duvel, J.-P., Ethé, C., Fairhead, L., Fichet, T., Flavoni, S., Friedlingstein, P., Grandpeix, J.-Y., Guez, L., Guilyardi, E., Hauglustaine, D., Hourdin, F., Idelkadi, A., Ghattas, J., Joussaume, S., Kageyama, M., Krinner, G., Labetoulle, S., Lahellec, A., Lefebvre, M.-P., Lefevre, F., Levy, C., Li, Z. X., Lloyd, J., Lott, F., Madec, G., Mancip, M., Marchand, M., Masson, S., Meurdesoif, Y., Mignot, J., Musat, I., Parouty, S., Polcher, J., Rio, C., Schulz, M., Swingedouw, D., Szopa, S., Talandier, C., Terray, P., Viovy, N., and Vuichard, N.: Climate change projections using the IPSL-CM5 Earth System Model: from CMIP3 to CMIP5, *Climate Dynamics*, 40, 2123–2165, doi:10.1007/s00382-012-1636-1, <https://link.springer.com/article/10.1007/s00382-012-1636-1>, 2013.
- 680 Dunić, N., Vilibić, I., Šepić, J., Somot, S., and Sevault, F.: Dense water formation and BiOS-induced variability in the Adriatic Sea simulated using an ocean regional circulation model, *Climate Dynamics*, doi:10.1007/s00382-016-3310-5, <http://link.springer.com/10.1007/s00382-016-3310-5>, 2016.
- Faugeras, B., Lévy, M., Mémerly, L., Verron, J., Blum, J., and Charpentier, I.: Can biogeochemical fluxes be recovered from nitrate and chlorophyll data? A case study assimilating data in the Northwestern Mediterranean Sea at the JGOFS-DYFAMED station, *Journal of Marine Systems*, 40-41, 99–125, doi:10.1016/S0924-7963(03)00015-0, <http://www.sciencedirect.com/science/article/pii/S0924796303000150>, 2003.
- 690 Fichaut, M., Garcia, M. J., Giorgetti, A., Iona, A., Kuznetsov, A., Rixen, M., and Group, M.: MEDAR/MEDATLAS 2002: A Mediterranean and Black Sea database for operational oceanography, in: Elsevier Oceanography Series, edited by H. Dahlin, K. Nittis and S. E. Petersson, N. C. F., vol. 69 of *Building the European Capacity in Operational Oceanography Proceedings of the Third International Conference on EuroGOOS*, pp. 645–648, Elsevier, <http://www.sciencedirect.com/science/article/pii/S0422989403801071>, 2003.
- Gibelin, A.-L. and Déqué, M.: Anthropogenic climate change over the Mediterranean region simulated by a global variable resolution model, *Climate Dynamics*, 20, 327–339, doi:10.1007/s00382-002-0277-1, <https://link.springer.com/article/10.1007/s00382-002-0277-1>, 2003.
- 700



- Giorgi, F.: Climate change hot-spots, *Geophysical Research Letters*, 33, L08 707, doi:10.1029/2006GL025734, <http://onlinelibrary.wiley.com/doi/10.1029/2006GL025734/abstract>, 2006.
- Giorgi, F. and Lionello, P.: Climate change projections for the Mediterranean region, *Global and Planetary Change*, 63, 90–104, doi:10.1016/j.gloplacha.2007.09.005, <http://www.sciencedirect.com/science/article/pii/S0921818107001750>, 2008.
- 705
- Gómez, F.: The role of the exchanges through the Strait of Gibraltar on the budget of elements in the Western Mediterranean Sea: consequences of human-induced modifications, *Marine Pollution Bulletin*, 46, 685–694, doi:10.1016/S0025-326X(03)00123-1, <http://www.sciencedirect.com/science/article/pii/S0025326X03001231>, 2003.
- 710
- Harley, C. D. G., Randall Hughes, A., Hultgren, K. M., Miner, B. G., Sorte, C. J. B., Thornber, C. S., Rodriguez, L. F., Tomanek, L., and Williams, S. L.: The impacts of climate change in coastal marine systems, *Ecology Letters*, 9, 228–241, doi:10.1111/j.1461-0248.2005.00871.x, <http://onlinelibrary.wiley.com/doi/10.1111/j.1461-0248.2005.00871.x/abstract>, 2006.
- Hattab, T., Albouy, C., Lasram, F. B. R., Somot, S., Le Loc'h, F., and Leprieux, F.: Towards a better understanding of potential impacts of climate change on marine species distribution: a multiscale modelling approach, *Global Ecology and Biogeography*, 23, 1417–1429, doi:10.1111/geb.12217, <http://onlinelibrary.wiley.com/doi/10.1111/geb.12217/abstract>, 2014.
- 715
- Herrmann, M., Sevault, F., Beuvier, J., and Somot, S.: What induced the exceptional 2005 convection event in the northwestern Mediterranean basin? Answers from a modeling study, *Journal of Geophysical Research: Oceans*, 115, C12 051, doi:10.1029/2010JC006162, <http://onlinelibrary.wiley.com/doi/10.1029/2010JC006162/abstract>, 2010.
- 720
- Herrmann, M., Diaz, F., Estournel, C., Marsaleix, P., and Ulses, C.: Impact of atmospheric and oceanic interannual variability on the Northwestern Mediterranean Sea pelagic planktonic ecosystem and associated carbon cycle, *Journal of Geophysical Research: Oceans*, 118, 5792–5813, doi:10.1002/jgrc.20405, <http://onlinelibrary.wiley.com/doi/10.1002/jgrc.20405/abstract>, 2013.
- 725
- Herrmann, M., Estournel, C., Adloff, F., and Diaz, F.: Impact of climate change on the northwestern Mediterranean Sea pelagic planktonic ecosystem and associated carbon cycle, *Journal of Geophysical Research: Oceans*, 119, 5815–5836, doi:10.1002/2014JC010016, <http://onlinelibrary.wiley.com/doi/10.1002/2014JC010016/abstract>, 2014.
- 730
- Huertas, I. E., Ríos, A. F., García-Lafuente, J., Navarro, G., Makaoui, A., Sánchez-Román, A., Rodríguez-Galvez, S., Orbi, A., Ruíz, J., and Pérez, F. F.: Atlantic forcing of the Mediterranean oligotrophy, *Global Biogeochemical Cycles*, 26, GB2022, doi:10.1029/2011GB004167, <http://onlinelibrary.wiley.com/doi/10.1029/2011GB004167/abstract>, 2012.
- Ibello, V., Cantoni, C., Cozzi, S., and Civitarese, G.: First basin-wide experimental results on N₂ fixation in the open Mediterranean Sea, *Geophysical Research Letters*, 37, L03 608, doi:10.1029/2009GL041635, <http://onlinelibrary.wiley.com/doi/10.1029/2009GL041635/abstract>, 2010.
- 735
- IPCC: *Managing the Risks of Extreme Events and Disasters to Advance Climate Change Adaptation. A Special Report of Working Groups I and II of the Intergovernmental Panel on Climate Change*, Cambridge University Press, Cambridge, United Kingdom, and New York, NY, USA, 2012.



- 740 IPCC and Working Group III: Emissions scenarios. a special report of IPCC Working Group III, Intergovernmental Panel on Climate Change, Geneva, <http://catalog.hathitrust.org/api/volumes/oclc/59436339.html>, oCLC: 891560334, 2000.
- Jordà, G., Marbà, N., and Duarte, C. M.: Mediterranean seagrass vulnerable to regional climate warming, *Nature Climate Change*, 2, 821–824, doi:10.1038/nclimate1533, <http://www.nature.com/nclimate/journal/v2/n11/abs/nclimate1533.html?foxtrotcallback=true>, 2012.
- 745 Klein, B., Roether, W., Kress, N., Manca, B. B., Ribera d'Alcala, M., Souvermezoglou, E., Theocharis, A., Civitarese, G., and Luchetta, A.: Accelerated oxygen consumption in eastern Mediterranean deep waters following the recent changes in thermohaline circulation, *Journal of Geophysical Research: Oceans*, 108, 8107, doi:10.1029/2002JC001454, <http://onlinelibrary.wiley.com/doi/10.1029/2002JC001454/abstract>, 2003.
- 750 Lascaratos, A., Roether, W., Nittis, K., and Klein, B.: Recent changes in deep water formation and spreading in the eastern Mediterranean Sea: a review, *Progress in Oceanography*, 44, 5–36, doi:10.1016/S0079-6611(99)00019-1, <http://www.sciencedirect.com/science/article/pii/S0079661199000191>, 1999.
- Lazzari, P., Mattia, G., Solidoro, C., Salon, S., Crise, A., Zavatarelli, M., Oddo, P., and Vichi, M.: The impacts of climate change and environmental management policies on the trophic regimes in the Mediterranean
- 755 Sea: Scenario analyses, *Journal of Marine Systems*, 135, 137–149, doi:10.1016/j.jmarsys.2013.06.005, <http://linkinghub.elsevier.com/retrieve/pii/S0924796313001425>, 2014.
- Lefort, S., Aumont, O., Bopp, L., Arsouze, T., Gehlen, M., and Maury, O.: Spatial and body-size dependent response of marine pelagic communities to projected global climate change, *Global Change Biology*, 21, 154–164, doi:10.1111/gcb.12679, <http://onlinelibrary.wiley.com/doi/10.1111/gcb.12679/abstract>, 2015.
- 760 Locarnini, R. A., Garcia, H. E., Boyer, T. P., Antonov, J. I., and Levitus, S.: World Ocean Atlas 2005, Volume 3: Dissolved Oxygen, Apparent Oxygen Utilization, and Oxygen Saturation [+DVD], NOAA Atlas NESDIS, <http://www.vliz.be/nl/imis?module=ref&refid=117383&printversion=1&dropIMISitle=1>, 2006.
- Ludwig, W., Dumont, E., Meybeck, M., and Heussner, S.: River discharges of water and nutrients to the Mediterranean and Black Sea: Major drivers for ecosystem changes during past and future decades?, *Progress in*
- 765 *Oceanography*, 80, 199–217, doi:10.1016/j.pocean.2009.02.001, <http://linkinghub.elsevier.com/retrieve/pii/S0079661109000020>, 2009.
- Ludwig, W., Bouwman, A. F., Dumont, E., and Lespinas, F.: Water and nutrient fluxes from major Mediterranean and Black Sea rivers: Past and future trends and their implications for the basin-scale budgets, *Global Biogeochemical Cycles*, 24, GB0A13, doi:10.1029/2009GB003594, <http://onlinelibrary.wiley.com/doi/10.1029/2009GB003594/abstract>, 2010.
- 770 Macias, D. M., Garcia-Gorritz, E., and Stips, A.: Productivity changes in the Mediterranean Sea for the twenty-first century in response to changes in the regional atmospheric forcing, *Frontiers in Marine Science*, 2, doi:10.3389/fmars.2015.00079, <https://www.frontiersin.org/articles/10.3389/fmars.2015.00079/full>, 2015.
- Madec, G.: NEMO ocean engine, <http://eprints.soton.ac.uk/64324/>, 2008.
- 775 Marty, J.-C., Chiavérini, J., Pizay, M. D., and Avril, B.: Seasonal and interannual dynamics of nutrients and phytoplankton pigments in the western Mediterranean Sea at the DYFAMED time-series station (1991–1999), *Deep-Sea Research, Part II. Topical Studies in Oceanography*, <http://www.vliz.be/en/imis?module=ref&refid=39389&printversion=1&dropIMISitle=1>, 2002.
- Monod, J.: Recherches sur la croissance des cultures bactériennes, Hermann, 1958.



- 780 Moutin, T., Van Wambeke, F., and Prieur, L.: Introduction to the Biogeochemistry from the Oligotrophic to the Ultraoligotrophic Mediterranean (BOUM) experiment, *Biogeosciences*, 9, 3817–3825, doi:10.5194/bg-9-3817-2012, <http://www.biogeosciences.net/9/3817/2012/>, 2012.
- Nabat, P., Somot, S., Mallet, M., Sevault, F., Chiacchio, M., and Wild, M.: Direct and semi-direct aerosol radiative effect on the Mediterranean climate variability using a coupled regional climate system model, *Climate Dynamics*, 44, 1127–1155, doi:10.1007/s00382-014-2205-6, <https://link.springer.com/article/10.1007/s00382-014-2205-6>, 2015.
- 785 Nittis, K., Lascaratos, A., and Theocharis, A.: Dense water formation in the Aegean Sea: Numerical simulations during the Eastern Mediterranean Transient, *Journal of Geophysical Research: Oceans*, 108, 8120, doi:10.1029/2002JC001352, <http://onlinelibrary.wiley.com/doi/10.1029/2002JC001352/abstract>, 2003.
- 790 Palmieri, J., Orr, J. C., Dutay, J.-C., Béranger, K., Schneider, A., Beuvier, J., and Somot, S.: Simulated anthropogenic CO₂ storage and acidification of the Mediterranean Sea, *Biogeosciences*, 12, 781–802, doi:10.5194/bg-12-781-2015, <http://www.biogeosciences.net/12/781/2015/>, 2015.
- Redfield, A. C., Ketchum, B. H., and Richards, F. A.: The influence of organisms on the composition of seawater, *The sea: ideas and observations on progress in the study of the seas*, <http://www.vliz.be/en/imis?module=ref&refid=28944&printversion=1&dropIMISitle=1>, 1963.
- 795 Richon, C., Dutay, J.-C., Dulac, F., Wang, R., Balkanski, Y., Nabat, P., Aumont, O., Desboeufs, K., Laurent, B., Guieu, C., Raimbault, P., and Beuvier, J.: Modeling the impacts of atmospheric deposition of nitrogen and desert dust-derived phosphorus on nutrients and biological budgets of the Mediterranean Sea, *Progress in Oceanography*, doi:10.1016/j.pocean.2017.04.009, <http://www.sciencedirect.com/science/article/pii/S0079661116301811>, 2017.
- 800 Richon, C., Dutay, J.-C., Dulac, F., Wang, R., and Balkanski, Y.: Modeling the biogeochemical impact of atmospheric phosphate deposition from desert dust and combustion sources to the Mediterranean Sea, *Biogeosciences*, 15, 2499–2524, doi:10.5194/bg-15-2499-2018, <https://www.biogeosciences.net/15/2499/2018/>, 2018.
- 805 Roether, W., Klein, B., and Hainbucher, D.: The Eastern Mediterranean Transient, in: *The Mediterranean Sea*, edited by Borzelli, G. L. E., Gačić, M., Lionello, P., and Paolalanotte-Rizzoli, pp. 75–83, John Wiley & Sons, Inc., <http://onlinelibrary.wiley.com/doi/10.1002/9781118847572.ch6/summary>, 2014.
- Rohling, E. J.: Shoaling of the Eastern Mediterranean Pycnocline due to reduction of excess evaporation: Implications for sapropel formation, *Paleoceanography*, 6, 747–753, doi:10.1029/91PA02455, <http://onlinelibrary.wiley.com/doi/10.1029/91PA02455/abstract>, 1991.
- 810 Rohling, E. J.: Review and new aspects concerning the formation of eastern Mediterranean sapropels, *Marine Geology*, 122, 1–28, doi:10.1016/0025-3227(94)90202-X, <http://www.sciencedirect.com/science/article/pii/002532279490202X>, 1994.
- Rossignol-Strick, M., Nesteroff, W., Olive, P., and Vergnaud-Grazzini, C.: After the deluge: Mediterranean stagnation and sapropel formation, *Nature*, 295, 105–110, doi:10.1038/295105a0, <http://www.nature.com/nature/journal/v295/n5845/abs/295105a0.html>, 1982.
- 815 Royer, J.-F., Cariolle, D., Chauvin, F., Déqué, M., Douville, H., Hu, R.-M., Planton, S., Rascol, A., Ricard, J.-L., Salas Y Melia, D., Sevault, F., Simon, P., Somot, S., Tyteca, S., Terray, L., and Valcke, S.: Simulation des changements climatiques au cours du XXI^e siècle incluant l’ozone stratosphérique, *Comptes Rendus Geo-*



- 820 science, 334, 147–154, doi:10.1016/S1631-0713(02)01728-5, <http://www.sciencedirect.com/science/article/pii/S1631071302017285>, 2002.
- Ruti, P. M., Somot, S., Giorgi, F., Dubois, C., Flaounas, E., Obermann, A., Dell'Aquila, A., Pisacane, G., Harzallah, A., Lombardi, E., Ahrens, B., Akhtar, N., Alias, A., Arsouze, T., Aznar, R., Bastin, S., Bartholy, J., Béranger, K., Beuvier, J., Bouffies-Cloch , S., Brauch, J., Cabos, W., Calmanti, S., Calvet, J.-C., Carillo, A., Conte, D., Coppola, E., Djurdjevic, V., Drobinski, P., Elizalde-Arellano, A., Gaertner, M., Gal n, P., 825 Gallardo, C., Gualdi, S., Goncalves, M., Jorba, O., Jord , G., L'Heveder, B., Lebeaupin-Brossier, C., Li, L., Liguori, G., Lionello, P., Maci s, D., Nabat, P.,  nol, B., Raikovic, B., Ramage, K., Sevault, F., Sannino, G., Struglia, M. V., Sanna, A., Torma, C., and Vervatis, V.: Med-CORDEX Initiative for Mediterranean Climate Studies, *Bulletin of the American Meteorological Society*, 97, 1187–1208, doi:10.1175/BAMS-D-830 14-00176.1, <https://journals.ametsoc.org/doi/abs/10.1175/BAMS-D-14-00176.1>, 2015.
- Schaap, D. M. and Lowry, R. K.: SeaDataNet – Pan-European infrastructure for marine and ocean data management: unified access to distributed data sets, *International Journal of Digital Earth*, 3, 50–69, doi:10.1080/17538941003660974, <http://www.tandfonline.com/doi/abs/10.1080/17538941003660974>, 2010.
- 835 Sevault, F., Somot, S., Alias, A., Dubois, C., Lebeaupin-Brossier, C., Nabat, P., Adloff, F., D qu , M., and Decharme, B.: A fully coupled Mediterranean regional climate system model: design and evaluation of the ocean component for the 1980–2012 period, *Tellus A*, 66, doi:10.3402/tellusa.v66.23967, <http://www.tellusa.net/index.php/tellusa/article/view/23967>, 2014.
- Somot, S., Sevault, F., and D qu , M.: Transient climate change scenario simulation of the Mediterranean Sea for the twenty-first century using a high-resolution ocean circulation model, *Climate Dynamics*, 27, 851–879, 840 doi:10.1007/s00382-006-0167-z, <http://link.springer.com/10.1007/s00382-006-0167-z>, 2006.
- Soto-Navarro, J., Somot, S., Sevault, F., Beuvier, J., Criado-Aldeanueva, F., Garc a-Lafuente, J., and B ranger, K.: Evaluation of regional ocean circulation models for the Mediterranean Sea at the Strait of Gibraltar: volume transport and thermohaline properties of the outflow, *Climate Dynamics*, 44, 1277–1292, 845 doi:10.1007/s00382-014-2179-4, <https://link.springer.com/article/10.1007/s00382-014-2179-4>, 2015.
- Takahashi, T., Broecker, W. S., and Langer, S.: Redfield ratio based on chemical data from isopycnal surfaces, *Journal of Geophysical Research: Oceans* (1978–2012), 90, 6907–6924, doi:10.1029/JC090iC04p06907, <http://onlinelibrary.wiley.com/doi/10.1029/JC090iC04p06907/abstract>, 1985.
- Taylor, K. E., Stouffer, R. J., and Meehl, G. A.: An Overview of CMIP5 and the Experiment Design, *Bulletin of the American Meteorological Society*, 93, 485–498, doi:10.1175/BAMS-D-11-00094.1, <http://journals.ametsoc.org/doi/abs/10.1175/BAMS-D-11-00094.1>, 2012.
- Theocharis, A., Nittis, K., Kontoyiannis, H., Papageorgiou, E., and Balopoulos, E.: Climatic changes in the Aegean Sea influence the eastern Mediterranean thermohaline circulation (1986–1997), *Geophysical Research Letters*, 26, 1617–1620, doi:10.1029/1999GL900320, <http://onlinelibrary.wiley.com/doi/10.1029/1999GL900320/abstract>, 1999. 855
- Vadsaria, T., Ramstein, G., Li, L., and Dutay, J.-C.: Sensibilit  d'un mod le oc an-atmosph re (LMDz-NEMOMED8)   un flux d'eau douce : cas du dernier  pisode de saprop le en mer M diterran e, *Quaternaire*, 28, 2017.



Velaoras, D. and Lascaratos, A.: North-Central Aegean Sea surface and intermediate water masses and
860 their role in triggering the Eastern Mediterranean Transient, *Journal of Marine Systems*, 83, 58–66,
doi:10.1016/j.jmarsys.2010.07.001, wOS:000282548300005, 2010.

Yogev, T., Rahav, E., Bar-Zeev, E., Man-Aharonovich, D., Stambler, N., Kress, N., Bèjà, O., Mulholland,
M. R., Herut, B., and Berman-Frank, I.: Is dinitrogen fixation significant in the Levantine Basin, East
Mediterranean Sea?, *Environmental Microbiology*, 13, 854–871, doi:10.1111/j.1462-2920.2010.02402.x,
865 <http://onlinelibrary.wiley.com/doi/10.1111/j.1462-2920.2010.02402.x/abstract>, 2011.



Name	Dynamics (NEMO years)	Buffer zone concentrations	River inputs
CTRL	1966–1981	1966–1981	1966–1981
CTRL_R	1966–1981	1966–1981	1980–2099
CTRL_RG	1966–1981	1980–2099	1980–2099
HIS/A2	1980–2099	1980–2099	1980–2099

Table 1. Description of the simulations. The years indicate the forcing years throughout the 120 years of simulation. The cycles are repeated in the CTRL simulations.

Simulation	Period	Whole Med.	Western	Eastern	Ionian-Levantine	Adriatic	Aegean	Atlantic buffer zone
HIS/A2	1980–1999	551	241	310	305	1.5	4.0	535
	2030–2049	570	240	329	324	1.4	3.6	543
	2080–2099	598	251	346	341	1.5	3.5	562
CTRL	1980–1999	545	238	307	302	1.6	4.0	532
	2030–2049	553	238	314	309	1.6	4.2	532
	2080–2099	560	241	319	313	1.7	4.2	532
CTRL_R	1980–1999	547	239	309	303	1.5	4.2	534
	2030–2049	536	232	304	299	1.4	3.5	534
	2080–2099	538	230	309	303	1.5	3.7	534
CTRL_RG	1980–1999	548	239	309	303	1.5	4.2	535
	2030–2049	536	233	303	298	1.4	3.5	544
	2080–2099	540	235	306	301	1.4	3.6	562

Table 2. Simulated integrated phosphate content (10^9 mol) over 20 years periods in the Mediterranean sub-basins in the different simulations. Basins are the same as defined in Fig.2 of Adloff et al. (2015), with the eastern basin including the Ionian, Levantine, Adriatic and Aegean subbasins.



Simulation	Period	Whole Med.	Western	Eastern	Ionian-Levantine	Adriatic	Aegean	Atlantic buffer zone
HIS/A2	1980–1999	13400	5520	7890	7690	66.9	132	8091
	2030–2049	13800	5450	8350	8100	88.5	163	8230
	2080–2099	14700	5750	8920	8650	98.3	164	8510
CTRL	1980–1999	13500	5530	7970	7760	66.2	144	8050
	2030–2049	12900	5320	7610	7420	61.7	131	8050
	2080–2099	12500	5170	7330	7150	58.7	123	8050
CTRL_R	1980–1999	13300	5470	7870	7760	66.8	138	8070
	2030–2049	13300	5250	8020	7770	88.0	162	8070
	2080–2099	13700	5300	8440	8170	94.2	177	8080
CTRL_RG	1980–1999	13300	5480	7870	7760	66.8	138	8090
	2030–2049	13300	5270	8010	7760	88.0	162	8080
	2080–2099	13800	5390	8430	8160	94.3	177	8080

Table 3. Simulated integrated nitrate content (10^9 mol) over 20 years periods in the Mediterranean sub-basins in the different simulations. Basins are the same as defined in Fig.2 of Adloff et al. (2015), with the eastern basin including the Ionian, Levantine, Adriatic and Aegean subbasins.

Simulation	Period	Whole Med.	Western	Eastern	Ionian-Levantine	Adriatic	Aegean	Atlantic buffer zone
HIS/A2	1980–1999	25700	9680	16000	13500	830	1720	3210
	2030–2049	23800	8980	14800	12700	720	1440	3280
	2080–2099	23400	9180	14300	12200	690	1390	3570
CTRL	1980–1999	27000	10200	16700	14200	880	1670	3180
	2030–2049	27000	10200	16900	14300	890	1710	3180
	2080–2099	26600	9980	16600	14000	880	1690	3180
CTRL_R	1980–1999	27000	10300	16700	14100	875	1720	3210
	2030–2049	26800	10100	16700	14300	780	1610	3210
	2080–2099	26400	9940	16500	14100	760	1600	3220
CTRL_RG	1980–1999	27000	10300	16700	14100	875	1720	3230
	2030–2049	26900	10200	16700	14300	780	1600	3260
	2080–2099	26700	10200	16500	14100	750	1600	3420

Table 4. Simulated integrated chlorophyll production (10^9 mol) over 20 years periods in the Mediterranean sub-basins in the different simulations. Basins are the same as defined in Fig.2 of Adloff et al. (2015), with the eastern basin including the Ionian, Levantine, Adriatic and Aegean subbasins.

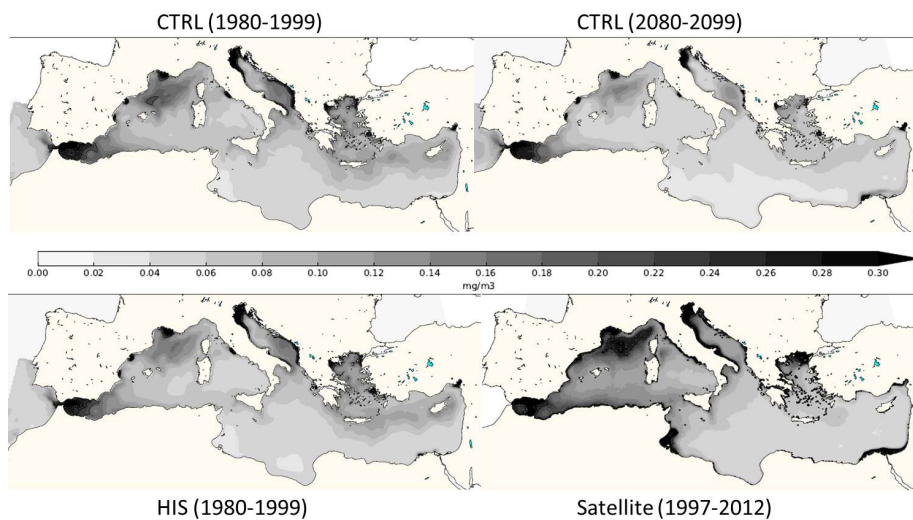


Figure 1. Average surface chlorophyll concentration from the CTRL (top, left: 1980–1999 right: 2080–2099) and HIS (bottom left) simulations, and from satellite estimations (MyOcean Dataset 1997–2012, bottom right).

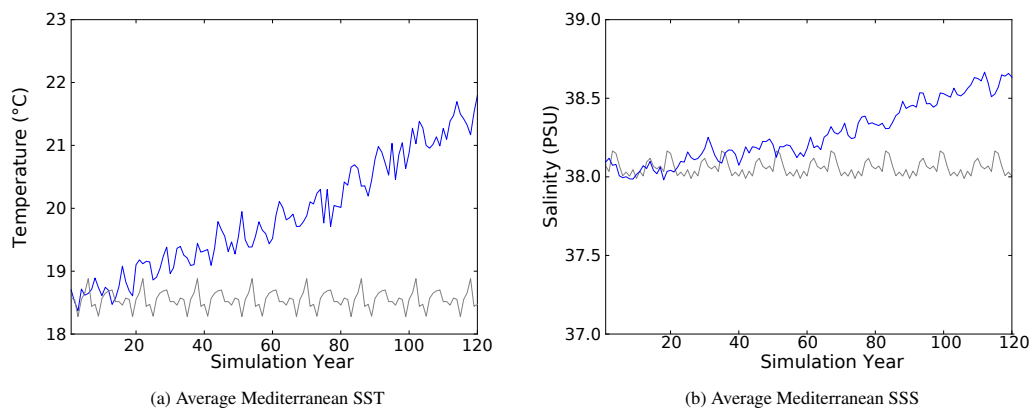


Figure 2. Evolution of average Mediterranean SST (left) and SSS (right) in CTRL (grey line) and HIS/A2 (blue line) simulations.

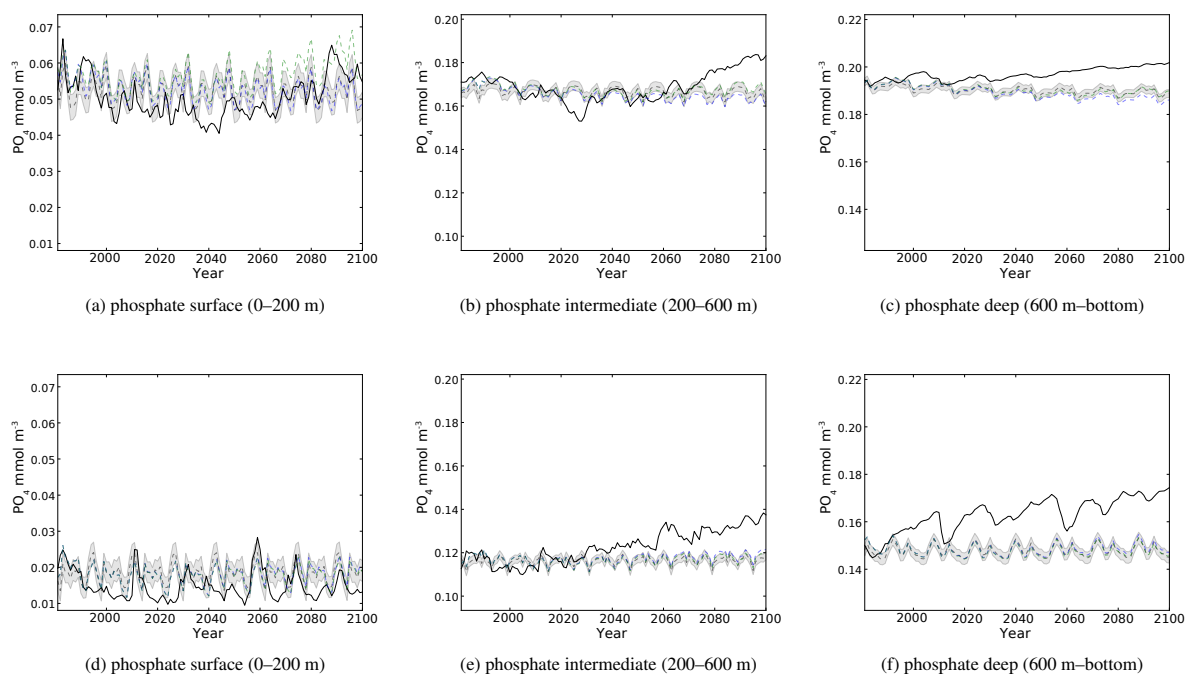


Figure 3. Evolution of yearly average phosphate concentration ($10^{-3} \text{ mol m}^{-3}$) in the surface (left), intermediate (middle) and bottom (right) layers in the western (top) and eastern (bottom) basin. Black line represent the HIS/A2 simulation, grey dashed line represent the CTRL (with standard deviation), dashed blue and green lines represent the CTRL_R and CTRL_RG simulations respectively.

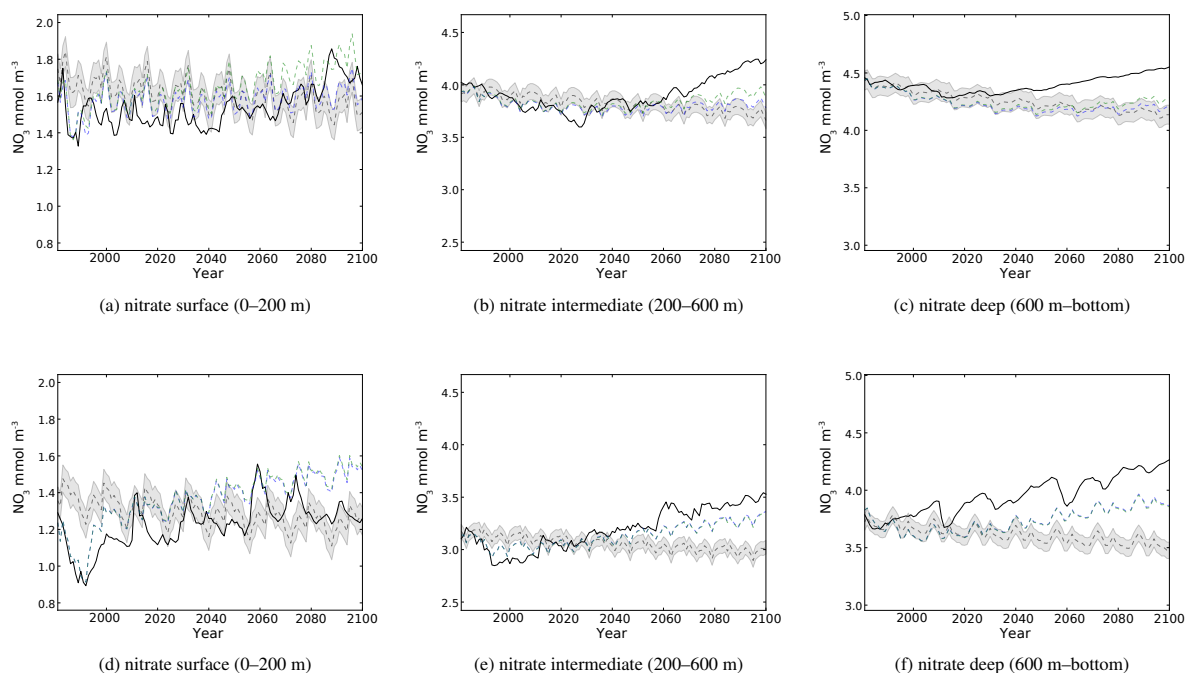


Figure 4. Evolution of yearly average nitrate concentration ($10^{-3} \text{mol m}^{-3}$) in the surface (left), intermediate (middle) and bottom (right) layers in the western (top) and eastern (bottom) basins. Black line represent the HIS/A2 simulation, grey dashed line represent the CTRL (with standard deviation), dashed blue and green lines represent the CTRL_R and CTRL_RG simulations respectively.

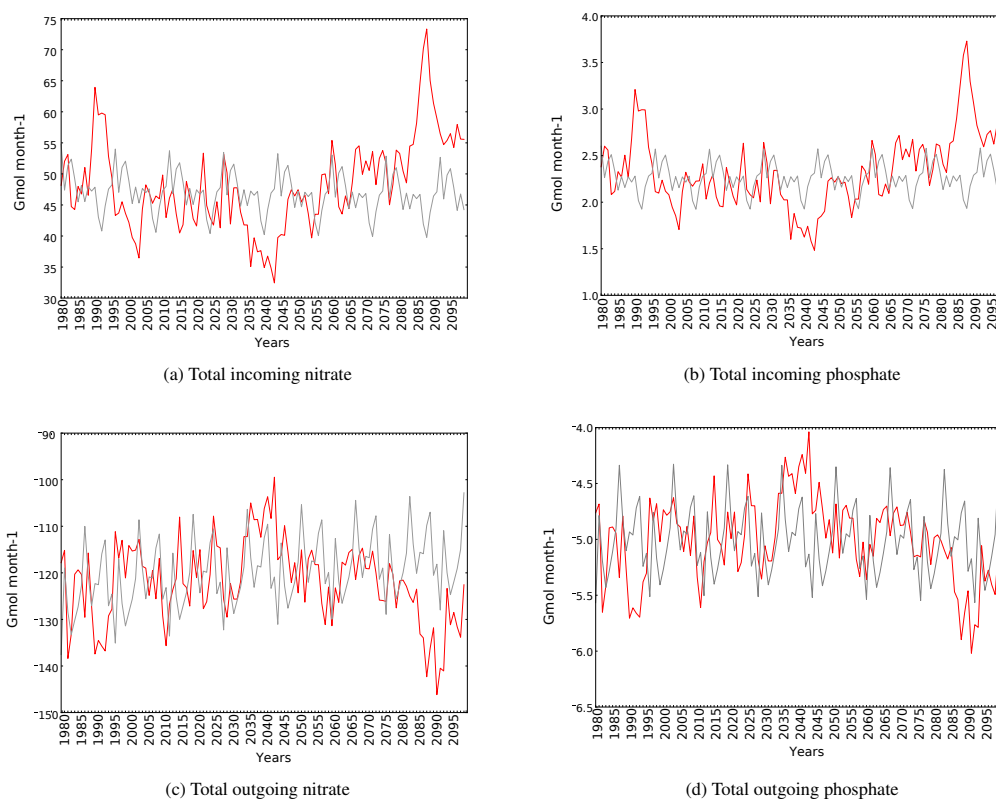


Figure 5. Evolution of total Gibraltar incoming (top) and outgoing (bottom) fluxes of nitrate and phosphate ($10^9 \text{ mol month}^{-1}$) in CTRL (grey line) and HIS/A2 (red line). Negative values indicate outgoing fluxes of nutrients.

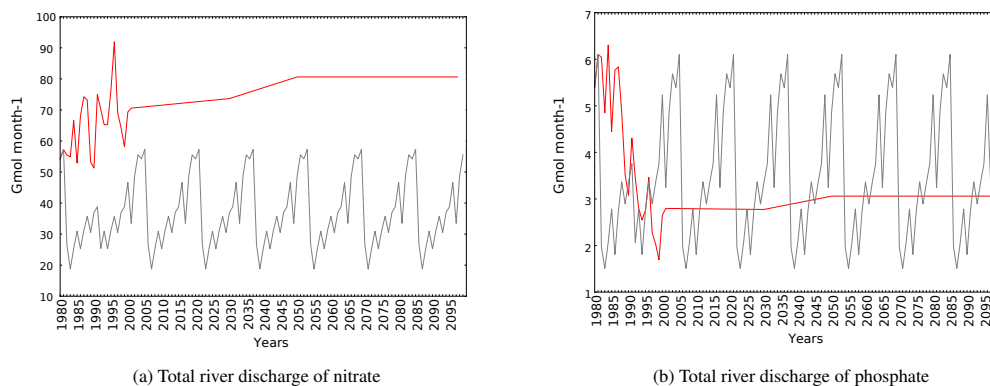


Figure 6. Evolution of total river discharge fluxes of nitrate and phosphate ($10^9 \text{ mol month}^{-1}$) to the Mediterranean Sea in CTRL (grey line) and HIS/A2 (red line).

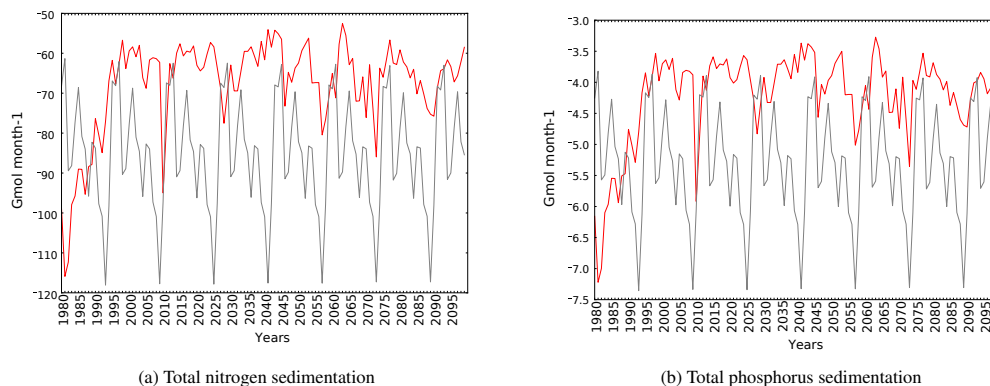


Figure 7. Evolution of total sedimentation fluxes of N and P ($10^9 \text{ mol month}^{-1}$) in the Mediterranean Sea in CTRL (grey line) and HIS/A2 (red line).

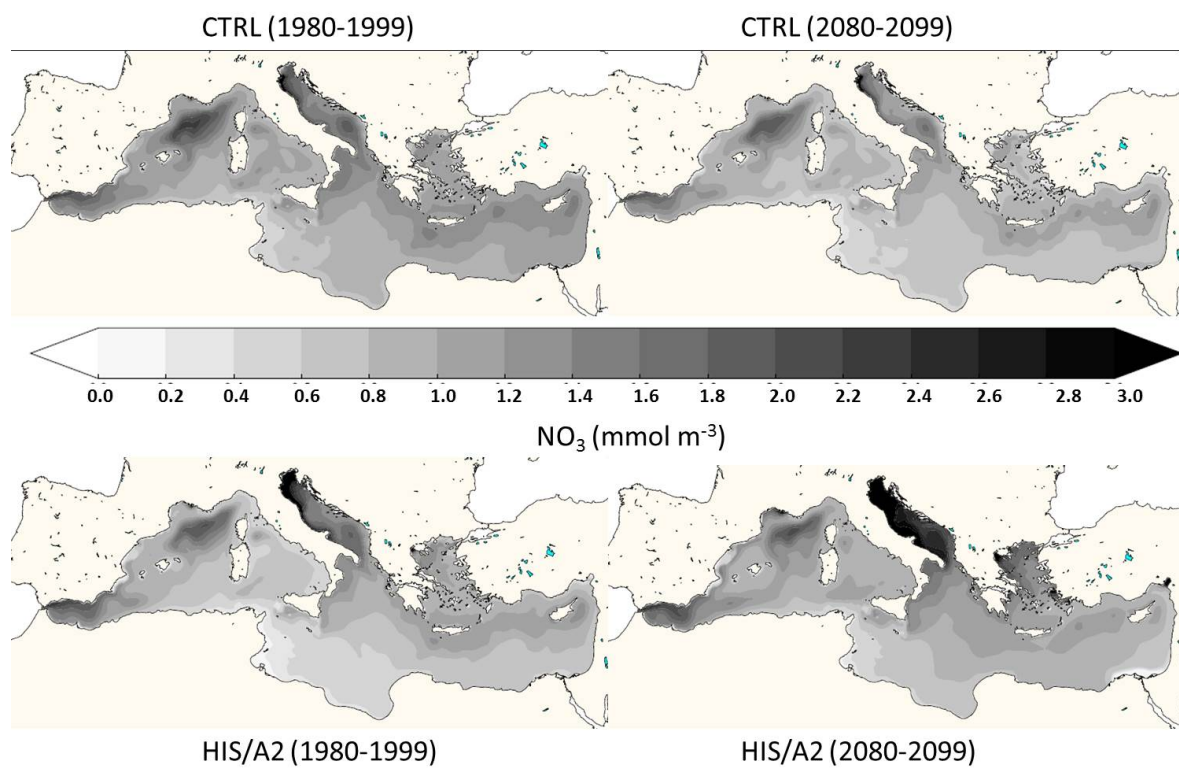


Figure 8. Present (1980–1999, left) and future (2080–2099, right) interannual average surface (0–200 m) concentrations of nitrate ($10^{-3} \text{ mol m}^{-3}$) in the CTRL (top) HIS/A2 (bottom) simulations.

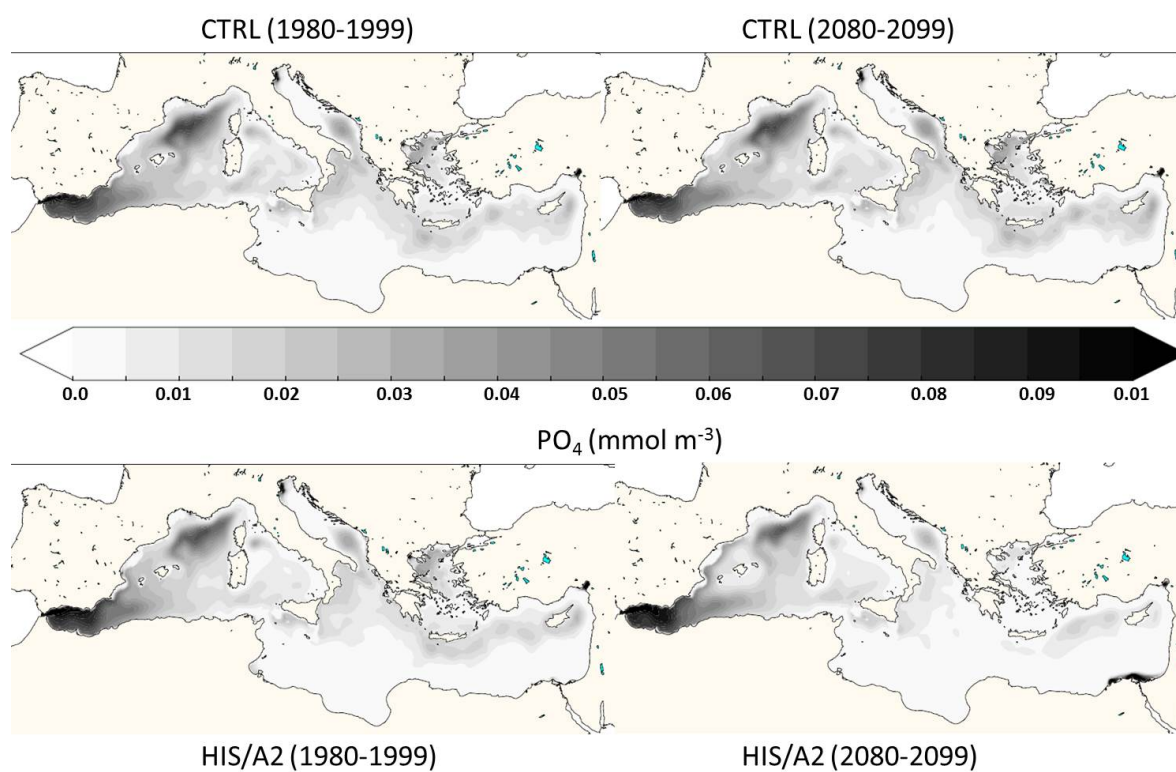


Figure 9. Present (1980–1999, left) and future (2080–2099, right) interannual average surface (0–200m) concentrations of phosphate ($10^{-3} \text{mol m}^{-3}$) in the CTRL (top) and HIS/A2 (right) simulations.

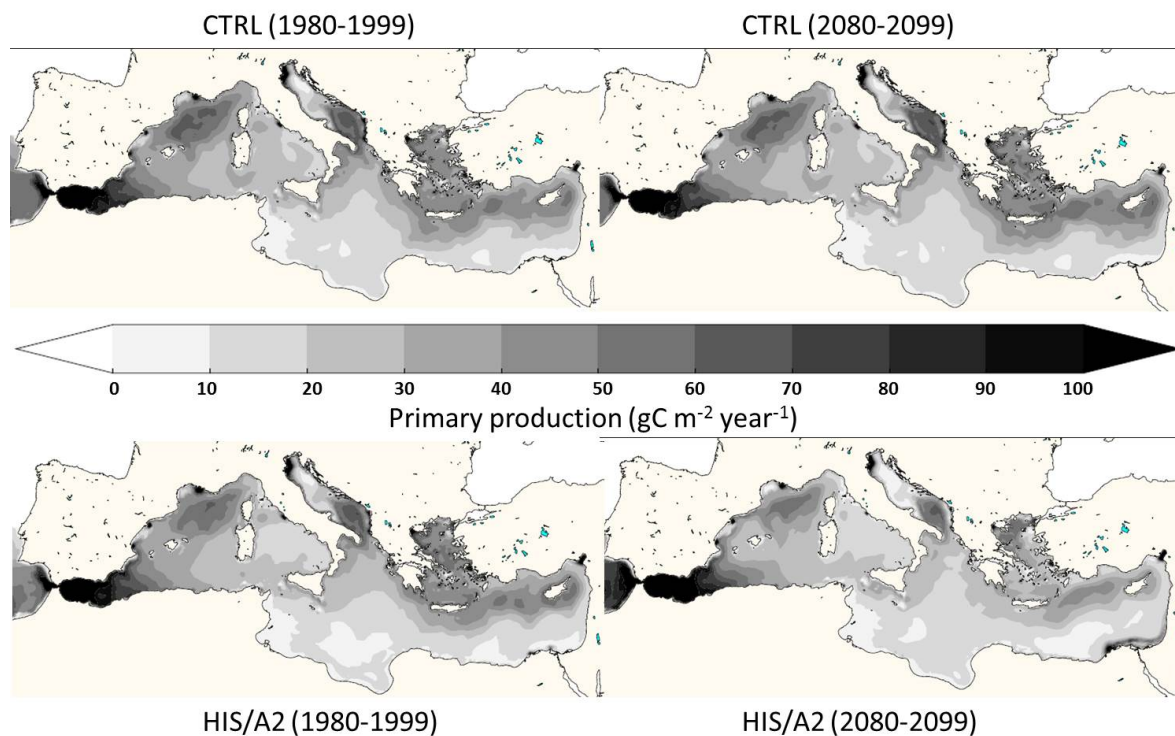


Figure 10. Present (1980–1999, left) and future (2080–2099, right) interannual average surface (0–200 m) integrated primary production (gC m^{-2}) in the CTRL (top) and HIS/A2 (bottom) simulations.

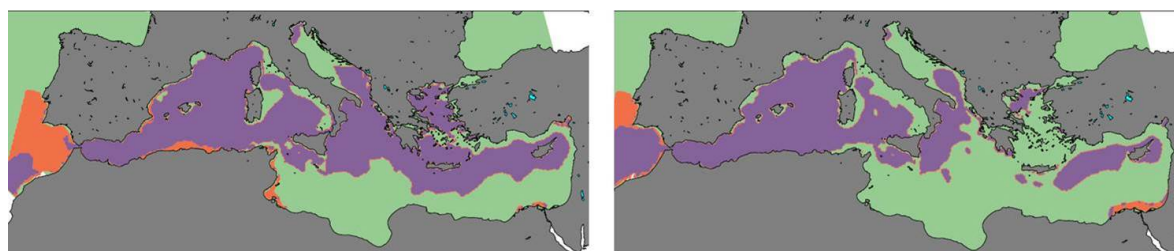


Figure 11. Present (1980–1999) and future (2080–2099) interannual average surface (0–200 m) limiting nutrient in the HIS/A2 simulation. N and P colimitation is considered when limitation factors for N and P differ by less than 1 %. Green zones are P-limited, Orange zones are N-limited and purple zones are N and P co-limited.

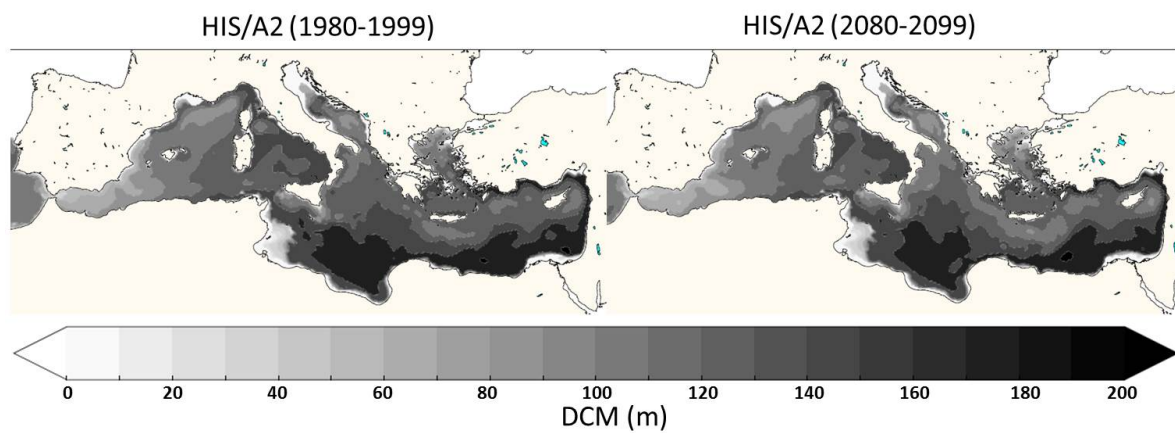


Figure 12. Present (left, 1980–1999) and future (right, 2080–2099) interannual average surface (0–200 m) DCM depth in the scenario simulation.

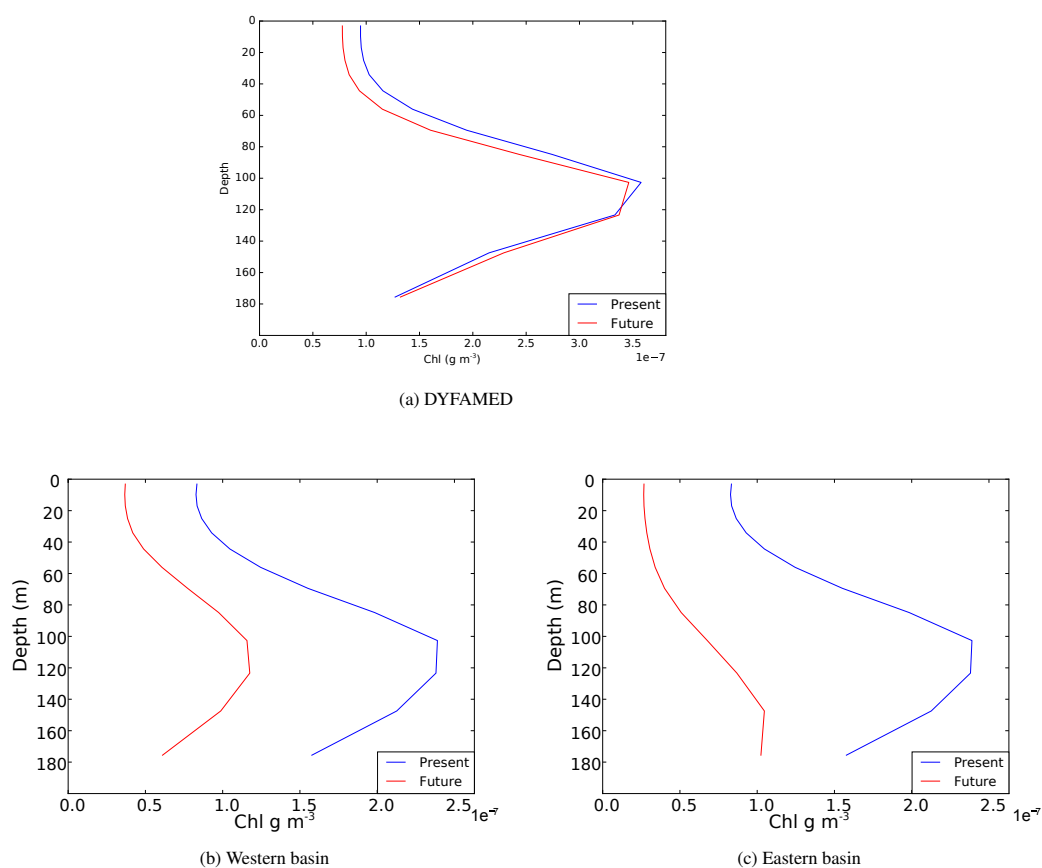


Figure 13. Present (1980–1999) and future (2080–2099) interannual average vertical profiles of total chlorophyll *a* ($10e^{-3}g m^{-3}$) at the DYFAMED station and averaged profiles over the western and eastern (including Aegean and Adriatic) basins.

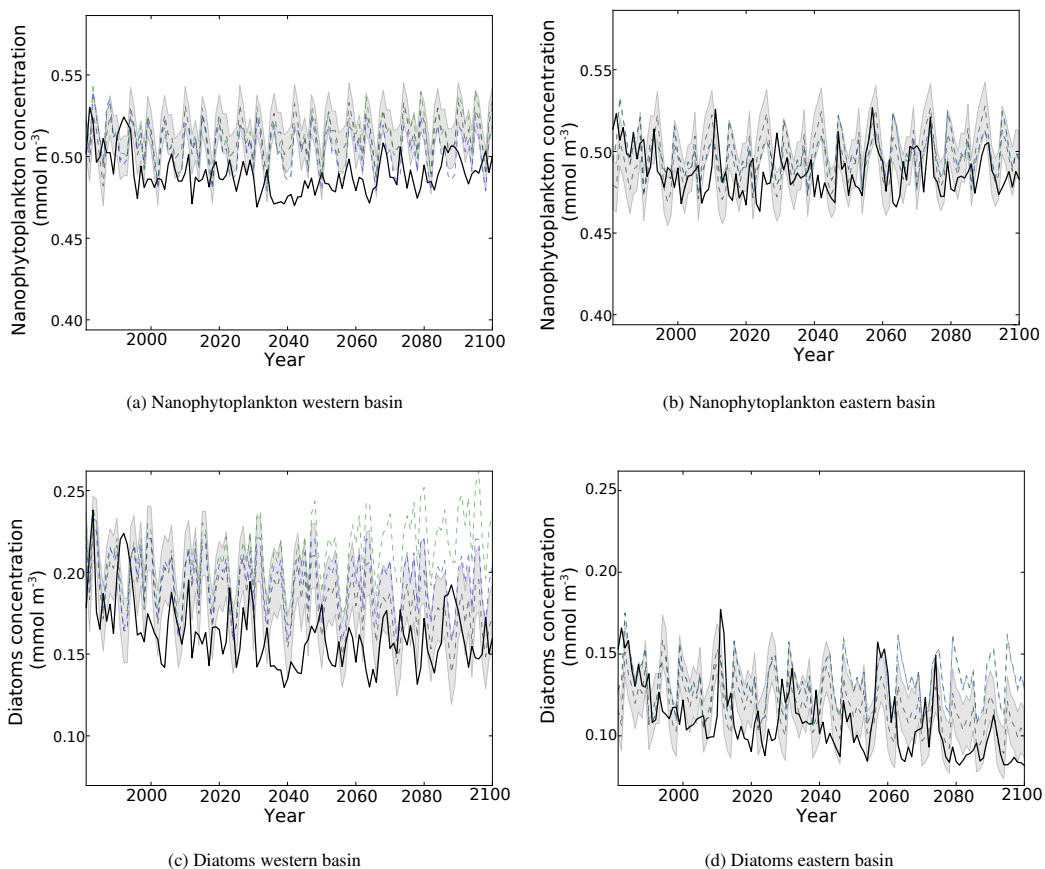


Figure 14. Evolution of yearly average nanophytoplankton and diatoms concentration ($10^{-3} \text{ mol m}^{-3}$) in the surface layer of the western and eastern basin. Black line represent the HIS/A2 simulation, grey dashed line represent the CTRL (with standard deviation), dashed blue and green lines represent the CTRL_R and CTRL_RG simulations respectively.

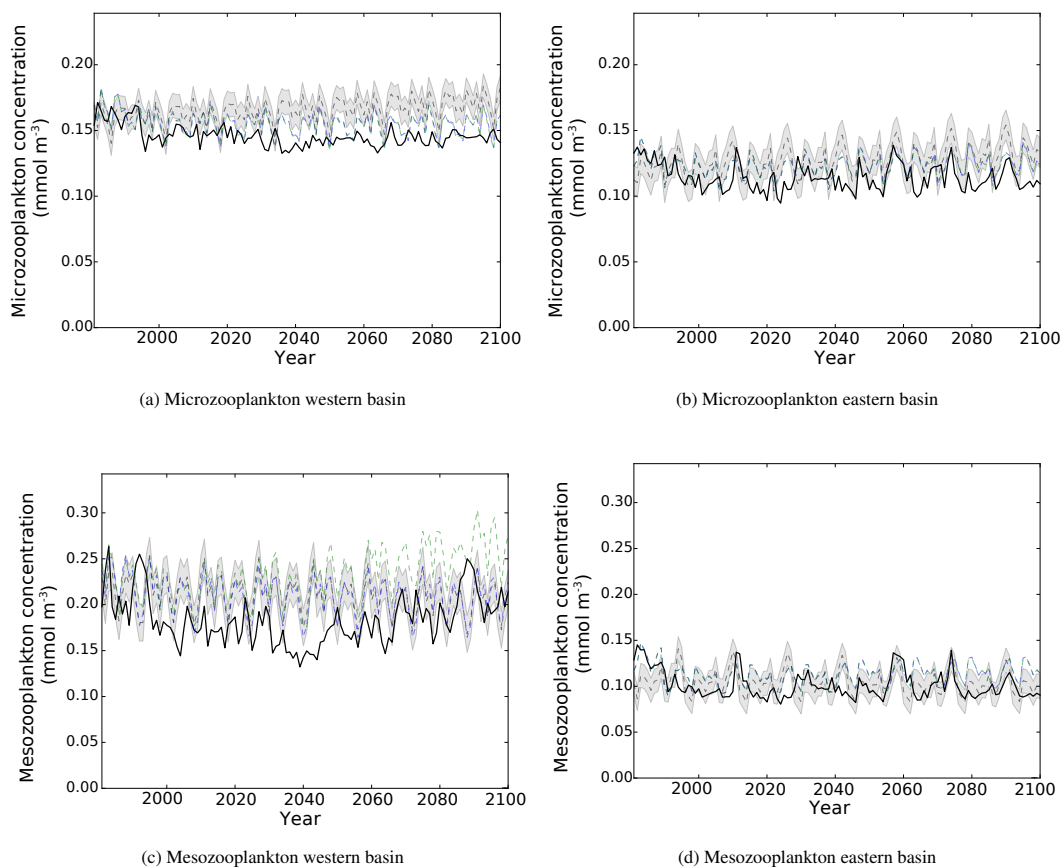


Figure 15. Evolution of yearly average microzooplankton and mesozooplankton concentrations ($10^{-3} \text{mol m}^{-3}$) in the surface layer of the western and eastern basins. Black line represent the HIS/A2 simulation, grey dashed line represent the CTRL (with standard deviation), dashed blue and green lines represent the CTRL_R and CTRL_RG simulations respectively.

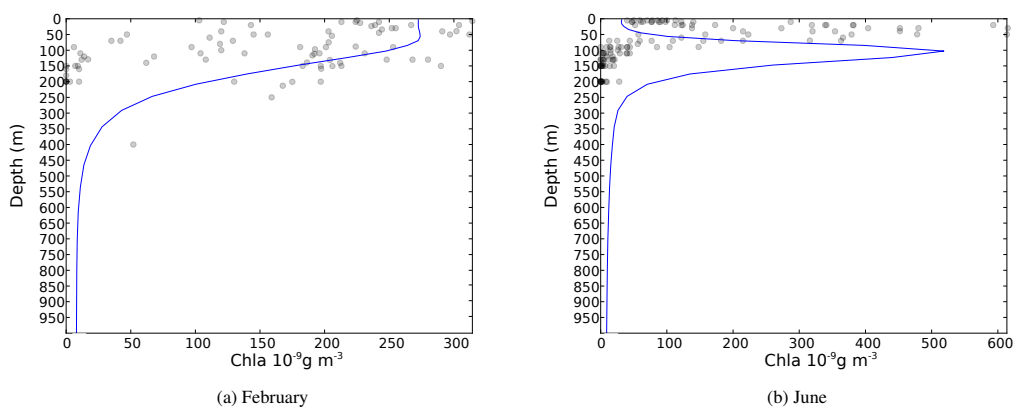
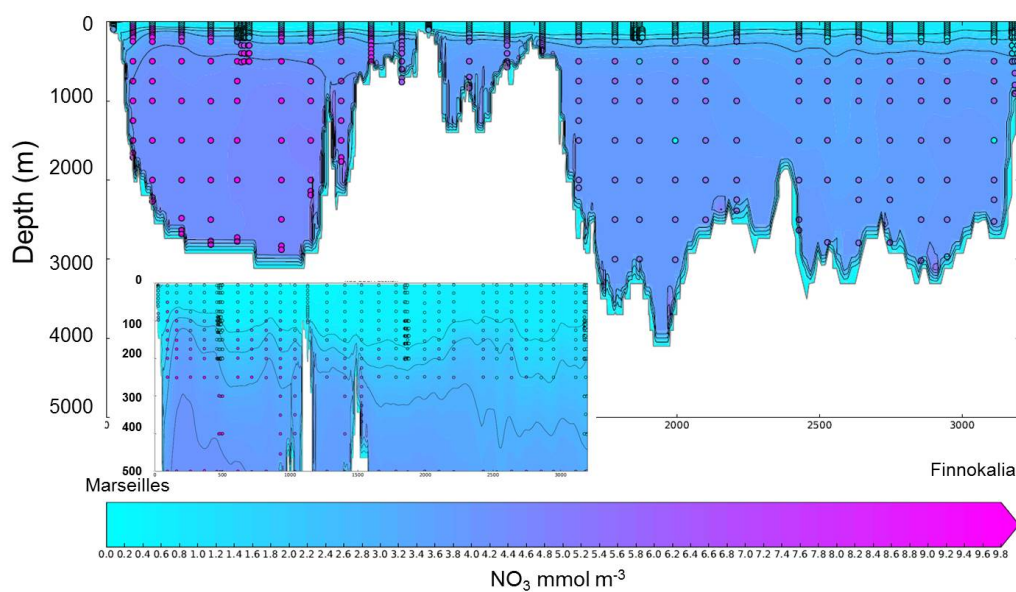
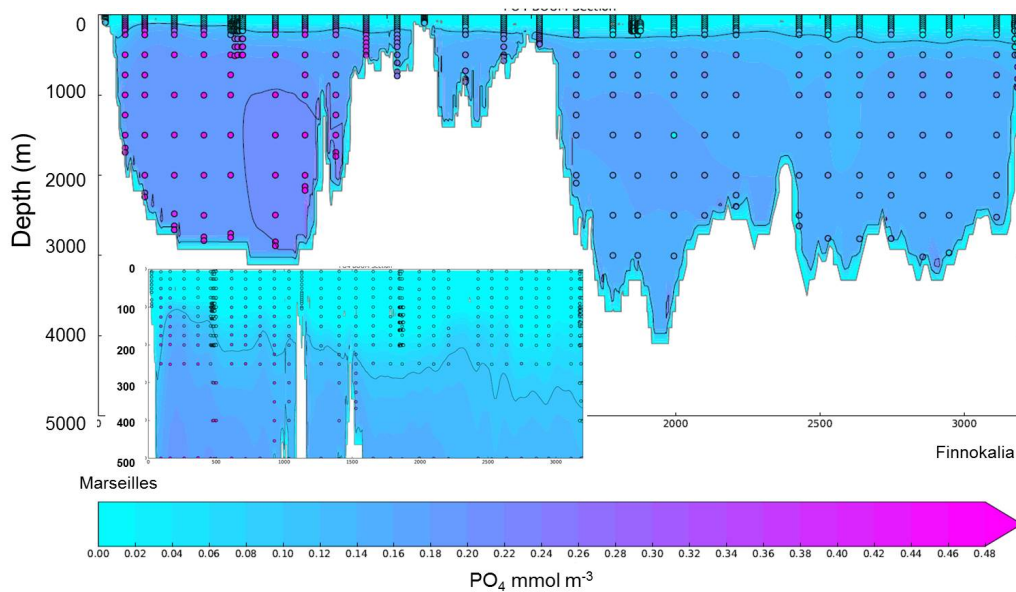


Figure A1. Average chlorophyll-a profiles in February (left) and June (right) for the first 20 years of the CTRL simulation at the DYFAMED station in the Ligurian Sea (43.4277°N, 7.2522°E). Dots represent data points (Marty et al., 2002; Faugeras et al., 2003).



(a) nitrate concentration



(b) P_4 concentration

Figure A2. Average concentrations of nitrate (top) and phosphate (bottom) for the 20 first years of the control simulation (CTRL). The dots represent data along a transect from Marseille to Finnokalia from the BOUM campaign (distances in km Moutin et al., 2012). The framed areas represent a vertical zoom of the top 500 m along the whole transect.